Collinear spin correlations of final-state radiation in dense QCD matter

João M. Silva, a,b,c Alba Soto-Ontoso

- ^a Departamento de Física Teórica y del Cosmos, Universidad de Granada, Campus de Fuentenueva, E-18071 Granada, Spain
- b Laboratório de Instrumentação e Física Experimental de Partículas (LIP), Av. Prof. Gama Pinto,
 2, 1649-003 Lisbon, Portugal

E-mail: joao.m.da.silva@tecnico.ulisboa.pt, aontoso@ugr.es

ABSTRACT: Spin correlations are required to reproduce the correct azimuthal dependence of matrix elements for successive branchings at disparate angles in QCD jets. In this paper, we study modifications to this, $\cos(2\psi_{12})$, azimuthal pattern in the presence of a quark-gluon plasma. To that end, we consider a simplified setup in which a narrow and energetic QCD antenna is formed inside a medium of fixed length and radiates a collinear emission outside it. The calculation includes both light and heavy-quarks. Further, we do not include medium-induced spin-flip interactions since they are energy suppressed in our formalism. We show that the amplitude of the azimuthal modulation in the presence of a medium is always suppressed with respect to the vacuum baseline, with its magnitude depending on the medium properties and splitting kinematics. For a medium with a momentum space anisotropy, we find that the azimuthal modulation acquires a phase shift, i.e., $\cos(2\psi_{12}) \rightarrow \cos(2\psi_{12} + \phi_{\rm med})$, where $\phi_{\rm med}$ is a process-dependent function that again depends on the medium properties and splitting kinematics. This work provides theory guidance for implementing spin-driven interference effects in phenomenological studies of jet quenching in heavy-ion collisions.

^cDepartamento de Física, Instituto Superior Técnico (IST), Universidade de Lisboa, Av. Rovisco Pais 1, 1049-001 Lisbon, Portugal

| Contents | | |
|----------|--|----|
| 1 | Introduction | 1 |
| 2 | Overview of collinear spin correlations in vacuum | 3 |
| | 2.1 Heuristic discussion | 3 |
| | 2.2 Cross-section computation | 5 |
| 3 | Collinear spin correlations in a QCD medium | 6 |
| | 3.1 Heuristic discussion | 6 |
| | 3.2 Amplitude in the BDMPS-Z formalism | 9 |
| | 3.3 Cross-section computation | 11 |
| 4 | Numerical results | 17 |
| | 4.1 Isotropic medium | 17 |
| | 4.2 Anisotropic medium | 19 |
| 5 | Conclusions | 22 |
| A | Calculation details | 23 |
| | A.1 Kinematics and phase-space parametrization | 23 |
| | A.2 Spin-dependent QCD vertices | 25 |
| | A.3 n -point medium averages in the large- N_c limit | 28 |

1 Introduction

The calculation of theoretical predictions for jet observables at collider experiments involves n-parton matrix-elements. QCD multiparton matrix elements adopt a particularly simple form in a variety of ordered limits, where kinematic properties of the emissions, such as their energy or angle, decrease from one emission to the next [1-4]. For instance, when all emissions are both soft and collinear, and widely separated in rapidity from each other, the tree-level n-parton matrix-element reduces to the product of n single-emission matrix-elements. This factorisation property lies at the core of parton shower algorithms [5].

Quantum interference effects driven by colour and spin degrees of freedom break this independent-emission picture. Colour interferences are relevant when considering multiple emissions at commensurate angles and strongly-ordered in energies. They lead to a suppression of soft, wide-angle emissions, i.e., the phenomenon of angular ordering of soft radiation [6–13]. Spin correlations appear when considering processes with intermediate off-shell gluons and become relevant for soft, wide-angle gluons that split collinearly or in successive collinear emissions strongly ordered in angle. In this work we focus on the latter.

These interference effects produce a non-trivial azimuthal correlation between the planes of consecutive emissions [14–28].

This paper studies spin-driven interference effects between successive QCD splittings when jet fragmentation evolves in a quark-gluon plasma (QGP) [29–36]. We will assume a weak-coupling description of the QGP, justified at high enough temperatures, so that perturbative QCD techniques, in particular the BDMPS-Z formalism [37–39], can be applied. The medium is then modeled as a stochastic, background colour field. This classical field contains information about both the colour density of the medium and the scattering potential that controls the interaction between the traversing partons and the medium. Considering all partons to be much more energetic than the relevant medium scales, spin-flip interactions are suppressed and thus the main effect of the medium is to colour-rotate the parton and to modify its transverse momentum distribution. The latter can be directional-dependent for some phenomenologically relevant scenarios in heavy-ion collisions. Examples of such cases are: strong longitudinal polarized fields in the glasma phase [40-44], anisotropic phasespace distributions in the pre-equilibrium phase [45–48] or matter gradients and flow in non-equilibrium QGP [49–58]. In this work, we will explore the case of a medium with a momentum space anisotropy for which rotational invariance is broken, while keeping the assumption of homogeneity [59–62].

The case of colour interferences has been studied in a series of works at the level of two-emissions using the antenna setup, where a first, energetic splitting then emits a soft gluon, either inside or outside the medium [63–75]. It has been observed that medium-interactions during both the antenna formation and its propagation modify the rate and phase-space of soft gluon emissions with respect to vacuum. In particular, colour exchanges between the antenna legs and the medium degrade the colour-correlation of the antenna and, eventually, lead to a fully decoherent state in which each of the legs radiate independently. Consequently, the regime where the two-emissions can be considered independent and thus the two-body matrix-element factorizes is actually enhanced with respect to vacuum.

On the other hand, the case of spin-driven interferences has never been explored. In this paper we compute the fully differential cross section for two collinear and strongly angular-ordered emissions. For simplicity, we take the second splitting to be outside of the medium, as the calculation of the full $1 \to 3$ matrix-element inside a QCD medium is considerably more involved [76–81]. Spin correlations between successive splittings only arise when there is an intermediate off-shell gluon, as a consequence of summing coherently over the spin states of this intermediate particle. Therefore, we restrict the calculation to processes like $a \to b \, g \to b \, c \, d$, where b, c, d can be either light quarks (q), heavy-quarks (Q) or gluons (g), i.e., $a, b, c, d \in (q, Q, g)$. In vacuum, the fully differential cross-section for such a configuration can be schematically written as

$$(2\pi)^2 \frac{d\sigma^{\text{vac}}}{dz_1 dz_2 d\theta_1 d\theta_2 d\phi_1 d\phi_2} = \frac{d\sigma^{\text{vac}}}{dz_1 d\theta_1} \frac{d\sigma^{\text{vac}}}{dz_2 d\theta_2} \left[1 + a\cos(2\psi_{12}) \right], \tag{1.1}$$

where $z_{1(2)}$ and $\theta_{1(2)}$ are the energy sharing fraction and the opening angle of the first (second) splitting, respectively. The deviation from the iterated emission picture is captured by the term in brackets in Eq. (1.1), where the coefficient $a(z_1, z_2, \theta_1, \theta_2)$ depends on the

final-state under consideration and its kinematics and $\psi_{12} = \phi_1 - \phi_2$ is the azimuthal difference between the planes spanned by the two branchings. We will come back to the exact definition of azimuthal angles below. The phenomenological implications of the azimuthal modulation in Eq. (1.1) have been discussed in, for instance, Refs. [22, 25, 26, 28, 82, 83].

The main result of this paper is that for a dense, anisotropic QCD medium the fully-differential cross-section reads

$$(2\pi)^{2} \frac{d\sigma^{\text{med}}}{dz_{1}dz_{2}d\theta_{1}d\theta_{2}d\phi_{1}d\phi_{2}} = \frac{d\sigma^{\text{vac}}}{dz_{1}d\theta_{1}} \frac{d\sigma^{\text{vac}}}{dz_{2}d\theta_{2}} (1 + F_{\text{med}}) \left[1 + a_{\text{med}} \cos(2\psi_{12} + \phi_{\text{med}}) \right], \quad (1.2)$$

where, in the vacuum limit, $1 + F_{\rm med} \to 1$, $a_{\rm med} \to a$ and $\phi_{\rm med} \to 0$ so that Eq. (1.2) reduces to Eq. (1.1). Medium modifications enter in three terms in the previous equation. First, $F_{\rm med}(E_a, z_1, \theta_1, \phi_1)$ is the same medium modification factor as the one introduced in Refs. [84, 85] and controls the nuclear modification to the antenna-formation cross-section. Second, $a_{\rm med} = a(z_1, z_2, \theta_1, \theta_2) f(E_a, z_1, \theta_1, \phi_1)$ suppresses the azimuthal modulation with respect to vacuum by a factor (f < 1) that depends on the phase-space point and the medium properties. Finally, medium interactions induce a phase-shift encoded by $\phi_{\rm med}$. In the isotropic case, since there is no preferred direction, this phase-shift vanishes together with the ϕ_1 dependence in $a_{\rm med}$. We highlight that Eq. (1.2) only holds when the second splitting happens outside the medium. If that were not the case both the factorised structure would be broken and the ψ_{12} -dependence would be more complex.

The rest of this paper is organized as follows. In Section 2, we discuss the regime of validity of our calculation and revisit the vacuum result. The differential cross-section for two-successive splittings including medium effects during the antenna formation and propagation is presented in Sec. 3. In Sec. 4, we present a numerical evaluation of the formulas obtained in 3 and we identify the regions of phase-space where medium effects are most relevant. We conclude in Sec. 5 with a summary and a discussion of the steps required to transform the present calculation into a phenomenological tool. Technical details on the calculation are reported in Appendix A.

2 Overview of collinear spin correlations in vacuum

2.1 Heuristic discussion

Before delving into the actual calculation, let us explain the kinematic regime in which the calculation is done and qualitatively discuss the emergence of spin-driven azimuthal correlations between subsequent splittings.

We consider $1 \to 3$ processes such as $a \to bg \to bcd$, i.e., any process with final-state partons b, c, d which includes an intermediate off-shell gluon that splits as $g \to cd$. We are interested in the limit where all final-state particles are *quasi*-collinear [86, 87]. Further,

¹This limit is a generalisation of the usual collinear limit [4], allowing for the definition of universal splitting functions that take mass effects into account [3, 87–89]. Put simply, one defines such a limit by taking all relative transverse momenta (or, equivalently, pair-wise angles) and on-shell masses to be small, while keeping their ratio fixed.

we shall consider this limit in the strongly-ordered regime where one enforces

$$\theta_2 \ll \theta_1 \ll 1$$
, $(\theta_1 \equiv \theta_{ba}, \theta_2 \equiv \theta_{cd})$ (2.1)

being θ_{ij} the opening angle of the ij pair of particles. In this strongly-ordered limit, the scattering amplitude for the $a \to b g \to b c d$ process factorizes into the production of a nearly on-shell gluon (\mathcal{M}_1) and its subsequent branching (\mathcal{M}_2) .² That is, the colour-stripped amplitude reads

$$i\mathcal{M}_{a\to cbd} \propto \sum_{\lambda_a,\lambda_c} \mathcal{M}_2^{\lambda_g \lambda_c \lambda_d}(p_c, p_d) \mathcal{M}_1^{\lambda_a \lambda_g \lambda_b}(p_b, p_g) \mathcal{M}_0^{\lambda_a}(p_a),$$
 (2.2)

where \mathcal{M}_0 is some initial production amplitude, $p_a = p_b + p_c + p_d$, $p_g = p_c + p_d$ and each \mathcal{M}_i is fully contracted in Dirac space and involves the propagator pole of the corresponding i-th splitting. The colour indices have been omitted for clarity and $\lambda_{a,b,c,d}$ are polarisation indices. The crucial point in Eq. (2.2) is that, despite \mathcal{M}_1 and \mathcal{M}_2 being factorised in Lorentz and Dirac indices, there is a coherent sum over physical polarisations λ_g , which upon squaring gives a double sum over polarisations, λ_g and λ'_g . The interference terms, i.e., when $\lambda_g \neq \lambda'_g$, result in a dependence on the relative azimuthal angle between the planes of the two consecutive splittings $\psi_{12} \equiv \phi_2 - \phi_1$ (see Eq. (A.7)).

To see this more clearly, we note that the dependence on azimuthal angles can be trivially factored out from each amplitude \mathcal{M}_i (see Appendix A.2), such that the amplitude can be written as

$$i\mathcal{M}_{a\to bg\to bcd} \propto \sum_{\lambda_g} \tilde{\mathcal{M}}_2^{\lambda_g \lambda_c \lambda_d}(z_2, |\boldsymbol{q}_2|) \tilde{\mathcal{M}}_1^{\lambda_a \lambda_g \lambda_b}(z_1, |\boldsymbol{q}_1|) \mathcal{M}_0(p_a)$$
$$\times e^{i(\lambda_g - \bar{\lambda}_c - \bar{\lambda}_d)\phi_2} e^{i(\bar{\lambda}_a - \lambda_g - \bar{\lambda}_b)\phi_1}, \tag{2.3}$$

where the barred polarisation indices are given by $\bar{\lambda} = \lambda$ if the particle is a gluon, and $\bar{\lambda} = \pm \lambda/2$ if the particle is a quark or an anti-quark, respectively. The light-cone energy fractions z_i and the relative transverse momenta of each splitting q_i are defined in Eq. (A.1) and the azimuthal angle of each splitting is defined as $\phi_i = \tan^{-1}(q_i^y/q_i^x)$. From Eq. (2.3), it is clear that, upon squaring the amplitude to obtain the cross-section, all azimuthal angle phases vanish except those proportional to λ_g , the intermediate gluon's polarisation state. Thus, the amplitude squared reads³

$$|\mathcal{M}_{a\to bg\to bcd}|^2 \propto |\mathcal{M}_0(p_a)|^2 \sum_{\lambda_g,\lambda_g'} F^{\lambda_g\lambda_g'}(z_i, |\boldsymbol{q}_i|) e^{i(\lambda_g - \lambda_g')\psi_{12}}, \qquad (2.4)$$

where

$$F^{\lambda_g \lambda_g'}(z_i, |\boldsymbol{q}_i|) = \frac{1}{2} \sum_{\lambda_a, \lambda_b, \lambda_c, \lambda_d} \tilde{\mathcal{M}}_2^{\lambda_g \lambda_c \lambda_d}(z_2, |\boldsymbol{q}_2|) \tilde{\mathcal{M}}_1^{\lambda_a \lambda_g \lambda_b}(z_1, |\boldsymbol{q}_1|) \times \left(\tilde{\mathcal{M}}_2^{\lambda_g' \lambda_c \lambda_d}(z_2, |\boldsymbol{q}_2|) \tilde{\mathcal{M}}_1^{\lambda_a \lambda_g' \lambda_b}(z_1, |\boldsymbol{q}_1|)\right)^*. \tag{2.5}$$

²Strictly speaking, one also needs the off-shell gluon to not take all the energy in $a \to b g$ for massless a and b and the splitting $g \to c d$ to not be highly asymmetric in energy for massive c and d. See e.g. Refs. [3, 89–91] for a more careful treatment of strongly ordered/"iterated" collinear limits.

³We assume that the initial parton is unpolarized, i.e., that \mathcal{M}_0 is spin independent. In doing so, we are discarding potential azimuthal correlations with initial-state particles.

Since $|\mathcal{M}|^2$ must be real, by defining $F^{\lambda_g \lambda_g'} = F_1^{\lambda_g} \delta^{\lambda_g, \lambda_g'} + F_2^{\lambda_g} \delta^{\lambda_g, -\lambda_g'}$ one can write

$$|\mathcal{M}_{a\to bcd}|^2 \propto |\mathcal{M}_0(p_a)|^2 \times \sum_{\lambda_g} \left[\operatorname{Re} F_1^{\lambda_g}(|\boldsymbol{q}_i|) + \operatorname{Re} F_2^{\lambda_g}(|\boldsymbol{q}_i|) \cos(2\psi_{12}) \right.$$
$$\left. - \lambda_g \operatorname{Im} F_2^{\lambda_g}(|\boldsymbol{q}_i|) \sin(2\psi_{12}) \right] . \tag{2.6}$$

At this stage we have isolated the azimuthal dependence into two terms proportional to $\cos(2\psi_{12})$ and $\sin(2\psi_{12})$. This dependence is simply a consequence of coherently summing over gluon polarisation states, since it comes from the terms with $\lambda'_g \neq \lambda_g$. In vacuum, the functions $F_i^{\lambda g}$ do not have an explicit polarisation dependence, i.e., $F_i^{\lambda g} = F_i$. Thus, the $\sin(2\psi_{12})$ term vanishes and we are left with a $\cos(2\psi_{12})$ modulation which is well known in the literature [15, 18, 19]. The phenomenological implications of this modulation have recently been studied in e.g. [22, 25, 26, 28, 82, 83].

2.2 Cross-section computation

Let us now explicitly calculate the azimuthal angle modulation of the vacuum cross-section for the process $a \to b \, g \to b \, c \, d$ in the strongly-ordered *quasi*-collinear limit. As already mentioned, in this limit the amplitude can be written as a product of propagator denominators and vertices that are fully contracted in Dirac and Lorentz indices

$$i\mathcal{M}_{a\to bcd} = \sum_{\lambda_g} \sum_{m,l} \left(\frac{i}{Q_g^2} ig T_{ij}^m V_{g\to cd}^{\lambda_g \lambda_c \lambda_d}(z_2, \boldsymbol{q}_2) \right) \left(\frac{i}{Q_a^2 - m_1^2} ig T_{kl}^m V_{a\to gb}^{\lambda_a \lambda_g \lambda_b}(z_1, \boldsymbol{q}_1) \right) \mathcal{M}_0^l(p_a),$$

$$(2.7)$$

where we explicitly sum over the colour and polarisation of the intermediate gluon and the colour of the initial parton a. For $q \to gq$ the colour matrices are in the fundamental representation $T_{kl}^m = t_{kl}^m$ while for $g \to gg$ one has the adjoint representation $T_{kl}^m = -if^{mkl}$. The vertices V are defined and calculated in Appendix A.2 and the propagator denominators are written in the collinear limit as a function of the virtuality

$$Q_a^2 - m_1^2 = p_a^2 - m_a^2 = \frac{q_1^2 + z_1^2 m_1^2}{z_1 (1 - z_1)} + \frac{q_2^2 + m_2^2}{z_1 z_2 (1 - z_2)} \approx \frac{q_1^2 + z_1^2 m_1^2}{z_1 (1 - z_1)},$$
 (2.8a)

$$Q_g^2 = (p_c + p_d)^2 = \frac{q_2^2 + m_2^2}{z_2(1 - z_2)},$$
(2.8b)

where m_i is the quark mass in the *i*-th splitting and in Eq. (2.8a) we imposed the strong ordering condition $\theta_1 \gg \theta_2$. Using the explicit vertex expressions in Appendix A.2, the squared matrix element summed over quantum numbers can be straightforwardly computed. To calculate the differential cross-section we then multiply by the appropriate phase-space element (see Eq. (A.12)), resulting in

$$(2\pi)^{2} \frac{d\sigma^{\text{vac}}}{\sigma_{0} d^{6}\Omega_{\text{PS}}} = \left(\frac{\alpha_{s}}{\pi}\right)^{2} C_{1} C_{2} \frac{P_{a \to bg}^{M}(z_{1}, \theta_{1})}{\theta_{1}(1 + \tilde{\theta}_{m,1}^{2})} \frac{P_{g \to cd}^{M}(z_{2}, \theta_{2})}{\theta_{2}(1 + \tilde{\theta}_{m,2}^{2})} [1 + a\cos(2\psi_{12})], \qquad (2.9)$$

which has the structure of Eq. (1.1) with

$$a \equiv S_{g \to cd} \frac{4z_2(1 - z_2)(1 - z_1)}{z_1[P_{a \to bq}(z_1) + z_1\tilde{\theta}_{m,1}^2][P_{q \to cd}(z_2) + \tilde{\theta}_{m,2}^2]}.$$
 (2.10)

The sign of a indicates whether spin correlations are enhanced when the two splittings occur in the same plane (a > 0) or in perpendicular planes (a < 0). The factor C_i is the colour factor associated to the i-th splitting, $S_{g \to gg} = +1$ and $S_{g \to q\bar{q}} = -1$. The functions $P^M_{i \to jk}$ are the spin-averaged massive splitting functions that read

$$P_{a\to bg}^{M}(z_1,\theta_1) = \frac{\theta_1^2 P_{a\to gb}(z_1) + z_1 \theta_{m,1}^2}{\theta_1^2 + \theta_{m,1}^2},$$
(2.11a)

$$P_{g\to cd}^{M}(z_2, \theta_2) = \frac{\theta_2^2 P_{g\to cd}(z_2) + \theta_{m,2}^2}{\theta_2^2 + \theta_{m,2}^2},$$
(2.11b)

with $P_{i\to jk}$ given by Eq. (A.23) and we have introduced dead-cone angles

$$\theta_{m,1} = \frac{m_1}{(1-z_1)E_a}, \qquad \theta_{m,2} = \frac{m_2}{z_1 z_2 (1-z_2)E_a},$$
(2.12)

and their ratios with respect to the opening angle of the splitting, i.e., $\tilde{\theta}_{m,i} \equiv \theta_{m,i}/\theta_i$. In Eq. (2.12), $E_a = p_a^+/\sqrt{2}$ is the energy of particle a. Finally, the initial production cross-section (see Eq. (A.12)) reads

$$\sigma_0 = \sum_{l} \int d^3 \Omega_a |\mathcal{M}_0^l(p_a)|^2. \tag{2.13}$$

Note that after integrating Eq. (2.9) over ϕ_1 and ψ_{12} we simply recover the product of the $a \to b g$ and $g \to c d$ massive splitting functions.

We evaluate the amplitude of the spin-modulation signal, i.e., Eq. (2.10), as a function of (z_1, z_2) in Fig. 1. In these results, $\theta_{m,1} = 0$. The left and right panels of Fig. 1 contain the $q \to qg \to qq'\bar{q}'$ and $g \to gg \to gq\bar{q}$ processes, respectively. The other relevant scale in Eq (2.10) is $\theta_{m,2}$. Since the massless case has been recently discussed [22, 25, 28], we focus on a massive $g \to Q\bar{Q}$ second splitting and choose $\tilde{\theta}_{m,2} = 0.1$ (top panels) and $\tilde{\theta}_{m,2} = 2$ (bottom panels). Let us first examine the top row where $\theta_{m,2} = 0.1$ and thus mass effects are suppressed. For both channels, we observe that the size of spin-correlations reaches its maximum around $z_1 \lesssim 0.1$ and $z_2 \sim 0.5$, i.e., when the initial parton is soft and the energy is shared democratically in the second branching. Comparing the two processes, we find that spin-correlations stay large for the q-initiated process in a wide region of phase-space. In fact, they only vanish when the two splittings are widely asymmetric, i.e., $z_{1,2} \to 0, 1$. For the g-initiated channel the spin modulation falls off much faster than in the quark case and becomes negligible when $z_1 \gtrsim 0.8$. The second row of Fig. 1 shows results for a second splitting whose opening angle is two-times smaller than the associated dead-cone angle and thus mass effects are expected to play a role, see Eq. (2.10). Indeed, we observe for both channels a significant depletion of spin-correlations by almost a factor 10.

3 Collinear spin correlations in a QCD medium

3.1 Heuristic discussion

Let us now consider the same process $a \to b g \to b c d$, in the strongly ordered quasi-collinear limit, inside a QCD medium. To simplify the calculation we take the $g \to c d$ splitting to

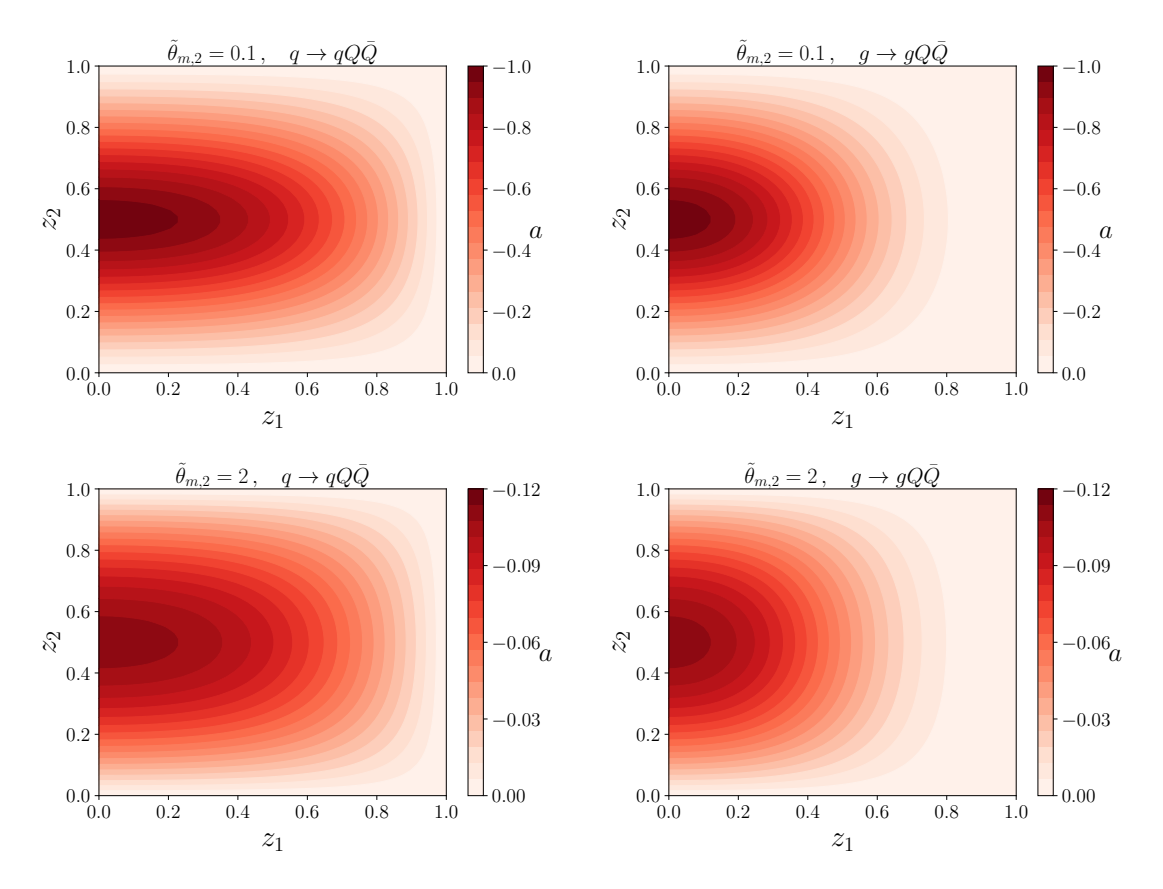


Figure 1: Amplitude of the spin modulation signal, a, defined in Eq. (2.10), as a function of both energy fractions z_i for two different first splittings (massless $q \to qg$ on the left and $g \to gg$ on the right), fixing the second splitting to be $g \to Q\bar{Q}$. From top to bottom we change the opening angle of the second splitting with respect to the dead-cone angle, i.e., $\tilde{\theta}_{m,2} = \theta_{m,2}/\theta_2$ with $\theta_{m,2}$ defined in Eq. (2.12).

be outside of the medium. Kinematically, this would correspond to a collinear splitting whose formation time is parametrically larger than the medium length, L. We describe the medium as a stochastic, coloured background field. At the amplitude level, each medium insertion yields a factor

$$igt^a \gamma^\mu \mathcal{A}^{a,\,\mu}(p^\mu) \,, \tag{3.1}$$

where g is the strong coupling, a a colour index and \mathcal{A} the classical background field. Every parton in the $a \to b \, g \to b \, c \, d$ splitting will interact with such field and thus the amplitude squared for the process is expected to be modified with respect to vacuum. Before carrying out the actual calculation of the in-medium amplitude, we discuss the analog of Eq. (2.6) for the medium case.

We consider partons with energies parametrically larger than any medium (e.g screening mass m_D) or transverse (relative to jet axis) scales. This means that parton-medium interactions do not significantly change the parton's virtuality, such that one can consider the intermediate gluon to stay nearly on-shell during its in-medium propagation. This hierarchy of

scales further implies that we can neglect spin-flip terms so that $\bar{u}(p,\lambda)\gamma^{\mu}u(p,\lambda')\approx 2p^{\mu}\delta^{\lambda,\lambda'}$. Hence, one can assume the form of the amplitude in Eq. (2.2) to hold

$$\int_{\boldsymbol{p}_a} |\mathcal{M}_{a \to bg \to bcd}^{\text{med}}|^2 \propto \sum_{\lambda_g, \lambda_g'} F_{\text{med}}^{\lambda_g \lambda_g'}(\boldsymbol{q}_1, \boldsymbol{q}_2) e^{i(\lambda_g - \lambda_g')\psi_{12}},$$
(3.2)

where we omitted the dependence on the remaining relevant variables, e.g. on z_i . The fact that in Eq. (3.2) the total transverse momentum dependence is integrated out is valid only for the case of transversely homogeneous media with instantaneous time correlations, see e.g. [92]. Unlike the vacuum case, $F_{\text{med}}^{\lambda_g \lambda_g'}(q_1, q_2)$ now depends not only on the moduli of the q_i vectors but also on their orientations. This means, in particular, that one should expect medium modifications to introduce a non-trivial dependence on the angle between planes ψ_{12} . Since we take the second splitting to be outside the medium, the q_2 dependence is given trivially by the vacuum expression for the second splitting

$$F_{\text{med}}^{\lambda_g \lambda_g'}(\boldsymbol{q}_1, \boldsymbol{q}_2) \underset{\text{in vacuum}}{\to} F_{\text{med}}^{\lambda_g \lambda_g'}(\boldsymbol{q}_1, |\boldsymbol{q}_2|). \tag{3.3}$$

We can now decompose $F_{\mathrm{med}}^{\lambda_g \lambda_g'}$ by projecting into the two possible helicity state combinations akin to the vacuum case, $F_{\mathrm{med}}^{\lambda_g \lambda_g'} = F_{\mathrm{med},1}^{\lambda_g} \delta^{\lambda_g \lambda_g'} + F_{\mathrm{med},2}^{\lambda_g} \delta^{\lambda_g,-\lambda_g'}$, and write the parametric dependence of the squared matrix element as

$$\int_{\boldsymbol{p}_{a}} |\mathcal{M}_{a \to bg \to bcd}^{\text{med}}|^{2} \propto \sum_{\lambda_{g}} \left[\operatorname{Re} F_{\text{med},1}^{\lambda_{g}}(\boldsymbol{q}_{1}, |\boldsymbol{q}_{2}|) + \operatorname{Re} F_{\text{med},2}^{\lambda_{g}}(\boldsymbol{q}_{1}, |\boldsymbol{q}_{2}|) \cos(2\psi_{12}) \right. \\
\left. - \lambda_{g} \operatorname{Im} F_{\text{med},2}^{\lambda_{g}}(\boldsymbol{q}_{1}, |\boldsymbol{q}_{2}|) \sin(2\psi_{12}) \right] . \tag{3.4}$$

We thus observe two major, qualitative modifications on the squared matrix-element with respect to vacuum: (i) it now depends on the orientation of q_1 , or equivalently on the value of ϕ_1 , and (ii) a potential non-zero $\sin(2\psi_{12})$ term if $F_{\text{med},2}^{\lambda_g}$ has a polarisation dependence. On top of these two effects, the dependence of $F_{\text{med},i}^{\lambda_g}$ on z_1 and $|q_1|$ can also be modified with respect to vacuum. As argued in App. A.2, effects (i) and (ii) are only realized for a medium model that is not rotationally invariant, e.g., a medium with some preferred axis, see Eq. (A.21). Thus, if one further considers an isotropic medium, the dependence on ϕ_1 and the $\sin(2\psi_{12})$ -term vanish and one is left with

$$\int_{\boldsymbol{p}_{a}} |\mathcal{M}_{a \to bg \to bcd}^{\text{med}}|^{2} \underset{\text{isotropic}}{\longrightarrow} \propto \sum_{\lambda_{g}} \left[\operatorname{Re} F_{\text{med},1}^{\lambda_{g}}(|\boldsymbol{q}_{1}|,|\boldsymbol{q}_{2}|) + \operatorname{Re} F_{\text{med},2}^{\lambda_{g}}(|\boldsymbol{q}_{1}|,|\boldsymbol{q}_{2}|) \cos(2\psi_{12}) \right].$$
(3.5)

To summarise: in an anisotropic medium, we expect a $\sin(2\psi_{12})$ -term together with a non-trivial dependence of the cross-section on ϕ_1 . In turn, for an isotropic medium, the azimuthal modulation is proportional to $\cos(2\psi_{12})$ as in vacuum, with both an overall modification and a change in the relative magnitude of the ψ_{12} -independent and $\cos(2\psi_{12})$ -terms that will depend on both the phase-space point of the first splitting and the medium properties. We calculate these functional dependencies explicitly in the following sections.

3.2 Amplitude in the BDMPS-Z formalism

Following the previous heuristic discussion, we now compute the medium modifications to the process $a \to b g \to b c d$, under the approximation that only the $a \to b g$ splitting occurs inside the medium and taking the medium to be static, homogeneous and of fixed length.

The problem of a highly energetic particle propagating in a dense QCD medium can be tackled within the perturbative BDMPS-Z approach $[37, 38]^4$, where one resums multiple scatterings with the medium at leading eikonal order, i.e., keeping the leading terms in powers of any transverse scale over the energy of the particle, while keeping sub-eikonal phases which are enhanced by the medium length and which are necessary to reproduce the Landau-Pomerachuk-Migdal effect [38, 94]. Thus, in a given diagram, each line in colour representation R is described by an effective non-relativistic quantum mechanical propagator, which in the light-cone gauge takes the form

$$G_R^{ij}(t_2, \boldsymbol{x}_2; t_1, \boldsymbol{x}_1 | p^+) = \int_{\boldsymbol{r}(t_1) = \boldsymbol{x}_1}^{\boldsymbol{r}(t_2) = \boldsymbol{x}_2} \mathcal{D}\boldsymbol{r}(t) \exp\left\{i\frac{p^+}{2} \int_{t_1}^{t_2} dt \, \dot{\boldsymbol{r}}^2\right\} U_R^{ij}(t_1, t_2, \boldsymbol{r}(t)), \quad (3.6)$$

with the endpoints denoting the starting and final transverse positions of the particle's evolution in light-cone time, $\mathbf{r}(t=x^+)$, at fixed light-cone energy p^+ . In the case of massive quarks one needs to account for mass dependent terms appearing in the propagator poles that lead to an additional sub-eikonal phase in Eq. (3.6) that depends on the quark mass m

$$G_F^{ij}(t_2, \boldsymbol{x}_2; t_1, \boldsymbol{x}_1 | p^+) \to G_F^{ij}(t_2, \boldsymbol{x}_2; t_1, \boldsymbol{x}_1 | p^+) \exp[-i\frac{m^2}{2p^+}(t_2 - t_1)].$$
 (3.7)

As mentioned in the previous section, we assume $p^+ \gg |\mathbf{p}|$, m, m_D to be the dominant scale of the problem, such that the relevant dynamics takes place in the plane transverse to the jet axis.⁵ Thus, the massive phase and the diffusive transverse motion dictated by the path integral are the leading sub-eikonal corrections. Further, the colour state of the parton is continuously rotated by successive scatterings with the medium and this is described by the path-ordered Wilson line

$$U_R^{ij}(x^+, y^+, \mathbf{r}) = \mathcal{P} \exp \left\{ ig \int_{x^+}^{y^+} ds^+ \mathcal{A}_a^-(s^+, \mathbf{r}(s^+)) T_{ij}^a \right\},$$
(3.8)

where $T_{ij}^a = t_{ij}^a$ if R = F (quark) and $T_{ij}^a = -if^{aij}$ if R = A (gluon). Here \mathcal{A} denotes an external classical field describing the underlying QCD background, as already introduced in Eq. (3.1). To calculate any amplitude at leading eikonal accuracy, the propagators of the form of Eq. (3.6) can be directly convoluted with the standard scalar QCD vertices (see App. A.2) such that, at tree level, one can use the same diagrams as in perturbation theory in the absence of a background medium, replacing the scalar particle propagators by in-medium propagators (cf. e.g. [61, 92, 93, 95]).

The classical field \mathcal{A} is induced by a stochastic distribution of colour sources of the background medium. As such, the computation of any in-medium process should involve

⁴See e.g. [30, 31, 34, 93] for recent reviews.

 $^{^5}$ Light-cone energy p^+ is conserved throughout the particle's in-medium propagation.

an average over possible configurations of colour sources. It is standard to assume that these configurations follow a Gaussian functional form, such that the only non-trivial average of \mathcal{A} fields is the two-point average given by [96, 97]

$$\langle \mathcal{A}_a^-(x^+, x^-, \boldsymbol{x}) \mathcal{A}_b^-(y^+, y^-, \boldsymbol{y}) \rangle = \delta_{ab} n(x^+, \boldsymbol{x}) \delta(x^+ - y^+) \gamma(\boldsymbol{x} - \boldsymbol{y}), \qquad (3.9)$$

which is local in colour and light-cone time. The form of field correlations is then set by $\gamma(\boldsymbol{x})$, which is directly related to the in-medium elastic scattering rate, and by the medium density $n(x^+, \boldsymbol{x})$, which for a static, fixed length and homogeneous medium is given by $n(x^+, \boldsymbol{x}) = n \Theta(x^+ < L^+)$, where $L = L^+/\sqrt{2}$ is usually of the order of a few fm. Hence, any in-medium cross-section involves an average of squared amplitudes according to Eq. (3.9).

Equipped with effective Feynman rules and a medium model we can now write the expression for the amplitude describing the $a \to b g \to b c d$ process. Consider particle a to be produced at fixed light-cone time $t_0 \equiv 0$ from an initial amplitude \mathcal{M}_0 , with fixed light-cone energy p_a^+ and fixed, arbitrary polarisation state. In the mixed space of light-cone time and transverse momentum, the amplitude for the process $a \to b g \to b c d$, where the splitting $g \to c d$ is imposed to happen outside of the medium, can be written as

$$i\mathcal{M} = \sum_{\lambda_{g}} \frac{e^{i\frac{\mathbf{p}_{b}^{2}}{2p_{b}^{+}}t_{\infty}}}{4p_{a}^{+}p_{g}^{+}} [igT_{ij}^{l}V_{g\to cd}^{\lambda_{g}\lambda_{c}\lambda_{d}}(z_{2}, \mathbf{q}_{2})] \int_{0}^{t_{\infty}} dt_{1} e^{-\varepsilon t_{1}} e^{i\frac{z_{1}^{2}m_{1}^{2}}{2\omega_{a}}t_{1}} \int_{t_{1}}^{t_{\infty}} dt_{2} e^{-\varepsilon t_{2}} \Theta(t_{2} > L)$$

$$\times e^{i(p_{c}^{-}+p_{d}^{-})t_{2}} \int_{\mathbf{k}_{b},\mathbf{k}_{g}} G_{A}^{lm}(t_{2}, \mathbf{p}_{g}; t_{1}, \mathbf{k}_{g}|p_{g}^{+}) G_{R_{a}}^{kn}(t_{\infty}, \mathbf{p}_{b}; t_{1}, \mathbf{k}_{b}|p_{b}^{+}) [igT_{np}^{m}V_{a\to gb}^{\lambda_{a}\lambda_{g}\lambda_{b}}(z_{1}, \mathbf{\kappa})]$$

$$\times \int_{\mathbf{p}_{0}} G_{R_{a}}^{pq}(t_{1}, \mathbf{k}_{0}; 0, \mathbf{p}_{0}|p_{a}^{+}) \mathcal{M}_{0}^{q}(\vec{p}_{0}),$$

$$(3.10)$$

where $T_{jk}^l = t_{jk}^l (-if^{ljk})$ in the fundamental (adjoint) representations and $R_a = F(A)$ if the initial particle is a quark (gluon). Most kinematic variables have been defined in Sec. 2, while the remaining ones are $p_c^- = (\boldsymbol{p}_c^2 + m_2^2)/(2p_c^+), p_d^- = (\boldsymbol{p}_d^2 + m_2^2)/(2p_d^+), \boldsymbol{p}_g = \boldsymbol{p}_c + \boldsymbol{p}_d$ and the intermediate momenta given by $\boldsymbol{k}_0 = \boldsymbol{k}_b + \boldsymbol{k}_g, \vec{p}_0 = (p_a^+, \boldsymbol{p}_0)$ and $\boldsymbol{\kappa} = (1-z_1)\boldsymbol{k}_g - z_1\boldsymbol{k}_b$. In our approximation, the light-cone energy is conserved, $p_0^+ = p_a^+$, but the total transverse momentum is not, $\boldsymbol{p}_0 \neq \boldsymbol{p}_a = \boldsymbol{p}_b + \boldsymbol{p}_c + \boldsymbol{p}_d$. Further, note that only the mass phases attached to the light-cone times of the vertices survive, since the final state ones cancel after being put on-shell. Finally, the ε -prescription ($\varepsilon \to 0$) assures that medium interactions are adiabatically turned off [39], such that one recovers the correct vacuum limit when taking $t_\infty \to +\infty$.

The integration variables t_1 and t_2 in Eq.(3.10) correspond to the light-cone times of the first and second splittings, respectively. As discussed, we take the second splitting to be outside the medium and so impose the condition $\Theta(t_2 > L)$ in Eq. (3.10). This restriction on the t_2 integral naturally ignores contributions to the medium modification which would only be included in the full $1 \to 3$ calculation inside the medium, which is considerably more involved. We thus expect our result to capture the correct qualitative behaviour in the case where there is a strong hierarchy on the formation time of the second splitting (τ_2)

with respect to the first splitting's (τ_1) and the medium length, i.e.,

$$\tau_2 \gg L, \, \tau_1, \quad \text{with} \quad \tau_1 \equiv 2p_a^+/(Q_a^2 - m_1^2), \, \tau_2 \equiv 2p_a^+/Q_a^2.$$
 (3.11)

Additionally, note that this restriction on the t_2 integration introduces spurious terms when trying to recover the vacuum limit at the amplitude level. Indeed, replacing all propagators by their vacuum counterpart, i.e.,

$$G_R^{ij} \to \delta^{ij} G_0(t_2, \mathbf{q}; t_1, \mathbf{p}|p^+) = \delta^{ij} e^{-i\frac{\mathbf{p}^2}{2p^+}(t_2 - t_1)} (2\pi)^2 \delta^2(\mathbf{q} - \mathbf{p}),$$
 (3.12)

leads to the following result

$$i\mathcal{M}_{a\to bcd} \underset{\text{limit}}{\xrightarrow{}} i\mathcal{M}_{a\to bcd}^{\text{vac}} \left[\frac{\tau_2}{\tau_2 - \tau_1} e^{iL/\tau_2} - \left(\frac{\tau_2}{\tau_2 - \tau_1} - 1 \right) e^{iL/\tau_1} \right],$$
 (3.13)

where $\mathcal{M}_{a\to bcd}^{\mathrm{vac}}$ is the vacuum amplitude calculated in Eq. (2.7). Hence, in order to recover the exact vacuum limit in Eq. (3.13) we conclude that we need to impose the same formation time hierarchy as in Eq. (3.11). As long as one does not have $z_1 \to 1$ (intermediate gluon taking all the energy on the first branching), this strong time-ordering is equivalent to the strong angular-ordering imposed in Eq. (2.1).

Finally, the light-cone time locality of the two-point average in Eq. (3.9) makes it convenient to separate the amplitude into two contributions: \mathcal{M}^{in} , where the first splitting is inside the medium, i.e., $t_1 \leq L$, and \mathcal{M}^{out} , where $t_1 > L$. The former contribution reads

$$i\mathcal{M}^{\text{in}} = \sum_{\lambda_g} \frac{e^{i\left(Q_a^2 - m_1^2 + \mathbf{p}_a^2\right)L/(2p_a^+)}}{2p_a^+} \left[\frac{i}{Q_g^2} igT_{ij}^l V_{g \to cd}^{\lambda_g \lambda_c \lambda_d}(z_2, \mathbf{q}_2) \right] \int_0^L dt_1 e^{-i\frac{z_1^2 m_1^2}{2\omega_a}(L - t_1)}$$

$$\times \int_{\mathbf{k}_b, \mathbf{k}_g, \mathbf{p}_0} G_A^{lm}(L, \mathbf{p}_g; t_1, \mathbf{k}_g | p_g^+) G_{R_a}^{kn}(L, \mathbf{p}_b; t_1, \mathbf{k}_b | p_b^+) [igT_{np}^m V_{a \to gb}^{\lambda_a \lambda_g \lambda_b}(z_1, \mathbf{\kappa})]$$

$$\times \int_{\mathbf{p}_0} G_{R_a}^{pq}(t_1, \mathbf{k}_0; 0, \mathbf{p}_0 | p_0^+) \mathcal{M}_0^q(\vec{p}_0),$$

$$(3.14)$$

while the latter is given by

$$i\mathcal{M}^{\text{out}} = \sum_{\lambda_g} e^{i\left(Q_a^2 - m_1^2 + \mathbf{p}_a^2\right)L/(2p_a^+)} \left[\frac{i}{Q_g^2} igT_{ij}^l V_{g \to cd}^{\lambda_g \lambda_c \lambda_d}(z_2, \mathbf{q}_2) \right] \left[\frac{i}{Q_a^2 - m_1^2} igT_{kp}^l V_{a \to gb}^{\lambda_a \lambda_b \lambda_g}(z_1, \mathbf{q}_1) \right]$$

$$\times \int_{\mathbf{p}_0} G_{R_a}^{pq}(L, \mathbf{p}_a; 0, \mathbf{p}_0 | p_a^+) \mathcal{M}_0^q(\vec{p}_0).$$

$$(3.15)$$

3.3 Cross-section computation

The fully differential in-medium cross-section for the process $a \to b g \to b c d$ is computed by first squaring the amplitude in Eq. (3.10). Following Eqs. (3.14),(3.15), we separate the calculation of the cross-section into time intervals according to

$$\mathcal{M}\mathcal{M}^{\dagger} = \mathcal{M}^{\text{in}}\mathcal{M}^{\text{in},\dagger} + 2\text{Re}\left(\mathcal{M}^{\text{in}}\mathcal{M}^{\text{out},\dagger}\right) + \mathcal{M}^{\text{out}}\mathcal{M}^{\text{out},\dagger}.$$
 (3.16)

The matrix-element squared then needs to be averaged over quantum numbers and over medium configurations ($\langle \cdot \rangle_{\mathcal{A}}$) according to Eq. (3.9). Combining this matrix-element with

the corresponding phase-space element in App. A.1, leads to the fully differential cross-section

$$\frac{16(2\pi)^6}{z_1^3(1-z_1)z_2(1-z_2)\theta_1\theta_2} \frac{d\sigma}{d^6\Omega_{\rm PS}} = \frac{1}{2} \int d^3\Omega_a(p_a^+)^4 \sum_{\rho_i,\lambda_i} \left\langle \mathcal{M} \mathcal{M}^{\dagger} \right\rangle_{\mathcal{A}}, \quad (3.17)$$

where the sum runs over colours (ρ_i) and spin states (λ_i) , and the factor 1/2 accounts for the average over the initial parton spin state.

Naturally, the term $d\sigma^{\text{out-out}}$ simply reduces to the vacuum result given by Eq. (2.9), since both splittings happen outside the medium and the broadening of the initial parton is integrated out due to the integration over total transverse momentum p_a . To compute the remaining terms, we note that from the medium-averaging point of view, only the first splitting matters, since the second occurs outside of the medium. We also adopt the large- N_c limit throughout the calculation. Then, Eq. (3.9) dictates that: (i) medium correlations are local in time and colour, and (ii) the medium is transversely homogeneous $(\gamma(x,y)=\gamma(x-y))$. Point (i) implies that the amplitude \mathcal{M} and its complex conjugate amplitude \mathcal{M}^{\dagger} form a colour singlet state at all times, while points (i) and (ii) imply that the total transverse momentum must be the same in \mathcal{M} and \mathcal{M}^{\dagger} at all times (cf. [92, 95]). Finally, by integrating over total momentum information (integral in $d^3\Omega_a$), the broadening of the initial parton a is integrated out and the squared initial production amplitude can be factored out. Thus, following a similar notation to [92], the $d\sigma^{\text{in-in}}$ and $d\sigma^{\text{in-out}}$ cross-section contributions read,

$$(2\pi)^{2} \frac{d\sigma^{\text{in-in}}}{\sigma_{0} d^{6}\Omega_{\text{PS}}} = \left(\frac{\alpha_{s}}{\pi}\right)^{2} \frac{C_{1}\theta_{1}}{8} \frac{C_{2}\omega_{g}^{2}\theta_{2}P_{g\to cd}^{M}(z_{2},\theta_{2})}{2z_{2}(1-z_{2})Q_{g}^{2}}$$

$$\times 2\text{Re} \int_{0}^{L} dt_{1} \int_{t_{1}}^{L} d\bar{t}_{1} e^{-i\frac{z_{1}^{2}m_{1}^{2}}{2\omega_{a}}(\bar{t}_{1}-t_{1})} \int_{\kappa,\bar{\kappa},l} Q_{a\to bg}(L,q_{1},q_{1};\bar{t}_{1},\bar{\kappa},l) \mathcal{K}_{a\to bg}(\bar{t}_{1},l;t_{1},\kappa)$$

$$\times \left[z_{1}^{3}m_{1}^{2} + P_{a\to gb}(z_{1}) \left(\kappa \cdot \bar{\kappa}\right) + S_{g\to cd} \frac{4z_{2}(1-z_{2})(1-z_{1})}{z_{1}(q_{2}^{2}P_{g\to cd}(z_{2}) + m_{2}^{2})} \left((q_{2} \cdot \kappa)(q_{2} \cdot \bar{\kappa})\right) - (q_{2} \times \kappa)_{z}(q_{2} \times \bar{\kappa})_{z}\right], \qquad (3.18a)$$

$$(2\pi)^{2} \frac{d\sigma^{\text{in-out}}}{\sigma_{0} d^{6}\Omega_{\text{PS}}} = -\left(\frac{\alpha_{s}}{\pi}\right)^{2} \frac{C_{1}\omega_{a}^{2}\theta_{1}}{2z_{1}(1-z_{1})(Q_{a}^{2}-m_{1}^{2})} \frac{C_{2}\omega_{g}^{2}\theta_{2}P_{g\to cd}^{M}(z_{2},\theta_{2})}{2z_{2}(1-z_{2})Q_{g}^{2}} \frac{1}{2\omega_{a}}$$

$$\times 2\text{Re} \ i \int_{0}^{L} dt_{1} e^{-i\frac{z_{1}^{2}m_{1}^{2}}{2\omega_{a}}(L-t_{1})} \int_{\kappa} \mathcal{K}_{a\to bg}(L,q_{1};t_{1},\kappa) \left[z_{1}^{3}m_{1}^{2} + P_{a\to gb}(z_{1}) \left(\kappa \cdot q_{1}\right) + S_{g\to cd} \frac{4z_{2}(1-z_{2})(1-z_{1})}{z_{1}(q_{2}^{2}P_{g\to cd}(z_{2}) + m_{2}^{2})} \left((q_{2} \cdot \kappa)(q_{2} \cdot q_{1}) - (q_{2} \times \kappa)_{z}(q_{2} \times q_{1})_{z}\right)\right], \qquad (3.18b)$$

where $(\mathbf{q}_2 \times \boldsymbol{\kappa})_z = q_2^x \kappa^y - q_2^y \kappa^x$ and, as in the vacuum case, $S_{g \to gg} = +1$ and $S_{g \to q\bar{q}} = -1$. Let us discuss some of the ingredients that enter into Eqs. (3.18a) and (3.18b). First, we observe that the vacuum splitting function for the second branching, $P_{g \to cd}^M$, appears. The terms within brackets inside the $\boldsymbol{\kappa}$ -integral correspond to the polarisation sum of the vertex product squared (see Eq. (A.22)). To factor out σ_0 (defined in Eq. (2.13)) we have assumed that \mathcal{M}_0 is sharply peaked around some value of energy p_a^+ . The objects \mathcal{K} and \mathcal{Q} , defined in App. A.3, involve only two-body (dipole) and four-body (quadrupole) medium averages, which is to be expected in the large- N_c limit (cf. [98, 99]). The latter can be written as a sum of a term with only dipoles ("factorizable") and a term containing quadrupoles ("non-factorizable") [84, 92, 95, 100]. In what follows, we shall neglect the "non-factorizable" piece⁶, which amounts to taking

$$Q_{a\to bg}(L, \boldsymbol{q}_1, \boldsymbol{q}_1; \bar{t}_1, \bar{\boldsymbol{\kappa}}, \boldsymbol{l}) \approx \delta^2(\boldsymbol{l} - \bar{\boldsymbol{\kappa}}) \int_{\boldsymbol{v}} e^{-i\boldsymbol{v}\cdot(\boldsymbol{q}_1 - \bar{\boldsymbol{\kappa}})} \mathcal{P}_{a\to gb}(L, \bar{t}_1, \boldsymbol{v}), \qquad (3.19)$$

where \mathcal{P} is a product of two dipole objects, describing the independent broadening of the intermediate gluon and parton b (see Eq. (A.29)). Under this approximation, all medium averages can be written as functions of products of dipole objects of the form

$$D(\bar{t}, t; \boldsymbol{u}) = \frac{1}{N_c} \left\langle \operatorname{Tr} \left(U_1^{\dagger} U_2 \right) \right\rangle = \exp \left\{ -\frac{C_F}{2} \int_t^{\bar{t}} ds \, n(s) \sigma(\boldsymbol{u}) \right\}, \quad \boldsymbol{u} = \boldsymbol{r}_1 - \boldsymbol{r}_2, \quad (3.20)$$

where $U_i^{jk} = U_F^{jk}(\bar{t}, t; \mathbf{r}_i)$ as defined in Eq. (3.8) and the dipole cross-section is written in terms of the scattering rate potential entering Eq. (3.9) as $\sigma(\mathbf{r}) = 2g^2(\gamma(0) - \gamma(\mathbf{r}))$.

Plugging Eq. (3.19) into Eqs. (3.18a),(3.18b) and performing the Fourier transforms to write everything in coordinate space we obtain:

$$(2\pi)^{2} \frac{d\sigma^{\text{in-in}}}{\sigma_{0} d^{6}\Omega_{PS}} = \left(\frac{\alpha_{s}}{\pi}\right)^{2} \frac{C_{1}\theta_{1}}{8} \frac{C_{2}\omega_{g}^{2}\theta_{2}P_{g\to cd}^{M}(z_{2},\theta_{2})}{2z_{2}(1-z_{2})Q_{g}^{2}}$$

$$\times 2\text{Re} \int_{0}^{L} dt_{1} \int_{t_{1}}^{L} d\bar{t}_{1}e^{-i\frac{z_{1}^{2}m_{1}^{2}}{2\omega_{a}}\Delta t} \int_{v} \left[z_{1}^{3}m_{1}^{2} + P_{a\to gb}(z_{1}) \left(\nabla_{u} \cdot \nabla_{\bar{u}}\right) - \right.$$

$$+ S_{g\to cd} \frac{4z_{2}(1-z_{2})(1-z_{1})}{z_{1}(q_{2}^{2}P_{g\to cd}(z_{2}) + m_{2}^{2})} \left((q_{2} \cdot \nabla_{u}) \left(q_{2} \cdot \nabla_{\bar{u}}\right) - \left(q_{2} \times \nabla_{u}\right)_{z} \left(q_{2} \times \nabla_{\bar{u}}\right)_{z}\right) \right]$$

$$\times e^{-iv \cdot q_{1}} \mathcal{P}_{a\to gb}(L, \bar{t}_{1}, v) \, \mathcal{K}_{a\to bg}(\bar{t}_{1}, \bar{u}; t_{1}, u)|_{u=0, \bar{u}=v} , \qquad (3.21a)$$

$$(2\pi)^{2} \frac{d\sigma^{\text{in-out}}}{\sigma_{0} d^{6}\Omega_{PS}} = \left(\frac{\alpha_{s}}{\pi}\right)^{2} \frac{C_{1}\omega_{a}^{2}\theta_{1}}{2z_{1}(1-z_{1})(Q_{a}^{2}-m_{1}^{2})} \frac{C_{2}\omega_{g}^{2}\theta_{2}P_{g\to cd}^{M}(z_{2}, \theta_{2})}{2z_{2}(1-z_{2})Q_{g}^{2}} \frac{1}{2\omega_{a}}$$

$$\times 2\text{Re} \int_{0}^{L} dt_{1}e^{-i\frac{z_{1}^{2}m_{1}^{2}}{2\omega_{a}}(L-t_{1})} \int_{v} \left[z_{1}^{3}m_{1}^{2} + P_{a\to gb}(z_{1}) \left(\nabla_{u} \cdot q_{1}\right) - \right.$$

$$+ S_{g\to cd} \frac{4z_{2}(1-z_{2})(1-z_{1})}{z_{1}(q_{2}^{2}P_{g\to cd}(z_{2}) + m_{2}^{2})} \left(\left(q_{2} \cdot \nabla_{u}\right) \left(q_{2} \cdot q_{1}\right) - \left(q_{2} \times \nabla_{u}\right)_{z} \left(q_{2} \times q_{1}\right)_{z}\right) \right]$$

$$\times e^{-iv \cdot q_{1}} \, \mathcal{K}_{a\to bg}(L, v; t_{1}, u)|_{u=0} . \qquad (3.21b)$$

At this point we have to provide an explicit form for the dipole cross-section $\sigma(r)$ entering the definition of the dipole medium average (3.20). In the multiple soft scattering

⁶This approximation was tested quantitatively in the context of $\gamma \to q\bar{q}$ [92]. It was concluded that the relative magnitude of the non-factorizable piece can get large when considering sufficiently large splitting angles $\theta \gtrsim 0.4$ and finite energy fractions $z \gtrsim 0.1$. Thus we expect the large- N_c result with only the factorizable piece to correctly capture the soft and collinear regime of the spectrum, while reasonably describing the main qualitative features of medium modifications outside of this region. Note that although the colour structure of $\gamma \to q\bar{q}$ is much simpler than that of pure QCD processes, this process still provides an indication of whether neglecting the non-factorizable contribution is reasonable. This is because at large- N_c the quadrupole arising from the 4-body average is common to all processes $\gamma \to q\bar{q}$, $q \to gq$ and $g \to gg$ (cf. e.g. [84, 95, 100]).

approximation one expands $\sigma(\mathbf{r})$ in the small distance limit, keeping only its quadratic dependence. Under such approximation, the potential is fully characterized by the jet quenching parameter \hat{q}^{7} , which in a medium with a momentum space anisotropy can take different values in the two directions orthogonal to the jet axis/initial particle's direction, i.e. $\hat{q}_x \neq \hat{q}_y$. This model for anisotropy has been implemented in this type of calculation in [60–62].⁸ For a static, finite length medium, the multiple soft scattering approximation takes the form

$$N_c \int_{t_1}^{t_2} dt \, n(s^+) \sigma(\mathbf{r}) = N_c(t_2 - t_1) \, n \, \sigma(\mathbf{r})$$

$$= \frac{t_2 - t_1}{2} \left(\hat{q}_x r_x^2 + \hat{q}_y r_y^2 \right) + \mathcal{O}(\mathbf{r}^2 \log(1/(m_D^2 \mathbf{r}^2))), \qquad (3.22)$$

where we have written the components of the transverse vector as $\mathbf{r} = (r_x, r_y)$ and m_D^{-1} sets a screening length for interactions. The broadening kernel can then be written as

$$\mathcal{P}_{a\to gb}(L, \bar{t}_1, \mathbf{v}) = \exp\left\{-\frac{1}{8} f_{a\to bg}(z_1)(L - \bar{t}_1)(\hat{q}_x v_x^2 + \hat{q}_y v_y^2)\right\}. \tag{3.23}$$

The splitting kernel $\mathcal{K}_{a\to bg}(\bar{t}_1, \boldsymbol{u}_2; t_1, \boldsymbol{u}_1)$ has a well known solution in the literature (see e.g. [100, 101])

$$\mathcal{K}_{a \to bg}(\bar{t}_1, \boldsymbol{u}_2; t_1, \boldsymbol{u}_1) = \sqrt{\frac{\omega_a \Omega_x}{2\pi i \sin \Omega_x \Delta t}} \exp \left\{ i \frac{\omega_a \Omega_x}{2 \sin \Omega_x \Delta t} \left[\left(u_{1x}^2 + u_{2x}^2 \right) \cos \Omega_x \Delta t - 2u_{1x} u_{2x} \right] \right\}$$

$$\times \sqrt{\frac{\omega_a \Omega_y}{2\pi i \sin \Omega_y \Delta t}} \exp \left\{ i \frac{\omega_a \Omega_y}{2 \sin \Omega_y \Delta t} \left[\left(u_{1y}^2 + u_{2y}^2 \right) \cos \Omega_y \Delta t - 2u_{1y} u_{2y} \right] \right\}, \tag{3.24}$$

with

$$\Omega_i = \left(\frac{1-i}{\sqrt{2}}\right) \sqrt{\frac{\hat{q}_i h_{a \to bg}(z_1)}{4\omega_a}}, \qquad \Delta t = \bar{t}_1 - t_1.$$
 (3.25)

The process dependent functions $f(z_1)$ and $h(z_1)$ read

$$f_{q \to gq}(z_1) = 2(1 - z_1)^2 + z_1^2$$
, $h_{q \to gq}(z_1) = 1 + (1 - z_1)^2$. (3.26a)

$$f_{g\to gg}(z_1) = 2[(1-z_1)^2 + z_1^2], \quad h_{g\to gg}(z_1) = 1 + z_1^2 + (1-z_1)^2.$$
 (3.26b)

Using the explicit form for the broadening and splitting kernels in Eqs. (3.23) and (3.24) and parametrizing the transverse momenta according to App. A.1, Eqs. (3.21a) and (3.21b) can be calculated analytically modulus integrations over light-cone times. We can then write the full spectrum in the following form

$$(2\pi)^{2} \frac{d\sigma^{\text{med}}}{\sigma_{0} d^{6}\Omega_{\text{PS}}} = \left(\frac{\alpha_{s}}{\pi}\right)^{2} C_{1} C_{2} \frac{P_{a \to bg}^{M}(z_{1}, \theta_{1})}{\theta_{1}(1 + \tilde{\theta}_{m,1}^{2})} \frac{P_{g \to cd}^{M}(z_{2}, \theta_{2})}{\theta_{2}(1 + \tilde{\theta}_{m,2}^{2})} (1 + F_{\text{med}}) \times \left[1 + a_{\text{med}} \cos(2\psi_{12} + \phi_{\text{med}})\right],$$
(3.27)

⁷Throughout this paper, we use \hat{q} in the adjoint representation.

⁸See e.g. Refs. [51, 52, 54–57] for different forms of including a medium with a non-trivial structure in a BDMPS-Z calculation.

where we observe (i) an overall modification of the spectrum encapsulated in the factor $1 + F_{\text{med}}$ [84, 92], (ii) a change in the modulation of the azimuth-dependent term (a_{med}) and (iii) a phase-shift (ϕ_{med}). These 3 factors depend on a series of auxiliary functions that we proceed to write down explicitly:

$$a_{\text{med}} = a \frac{\sqrt{A_1^2 + A_2^2}}{1 + F_{\text{med}}},$$
 (3.28a)

$$\tan \phi_{\text{med}} = \frac{A_2}{A_1}, \tag{3.28b}$$

where a corresponds to the amplitude of spin correlations in vacuum, see Eq. (2.10). The auxiliary functions A_1 , A_2 and F_{med} are given by

$$F_{\text{med}} = \frac{1}{\omega_{a} P_{a \to bg}^{M}(z_{1}, \theta_{1})} 2 \operatorname{Re} i \left\{ \int_{0}^{L} dt_{1} e^{-i\frac{z_{1}^{2}m_{1}^{2}}{2\omega_{a}}(L - t_{1})} e^{-i\frac{q_{1}^{2}}{2\omega_{a}} \left(\frac{\cos^{2} \phi_{1}}{c_{2}x} + \frac{\sin^{2} \phi_{1}}{c_{2}y}\right)} \frac{\sqrt{c_{1x}}\sqrt{c_{1y}}}{\sqrt{c_{2x}}\sqrt{c_{2y}}} \right. \\
\times \left[z_{1}^{3} m_{1}^{2} + P_{a \to gb}(z_{1}) \left(\mathcal{D}_{+} + \mathcal{D}_{-} \cos(2\phi_{1}) \right) \right] - \left(\frac{Q_{a}^{2} - m_{1}^{2}}{2p_{a}^{+}} \right) \int_{0}^{L} dt_{1} \int_{t_{1}}^{L} d\bar{t}_{1} e^{-i\frac{z_{1}^{2}m_{1}^{2}}{2\omega_{a}}\Delta t} \\
\times e^{i\frac{q_{1}^{2}}{2\omega_{a}} \left(\frac{\cos^{2} \phi_{1}}{c_{3x}} + \frac{\sin^{2} \phi_{1}}{c_{3y}} \right)} \frac{\sqrt{c_{1x}}\sqrt{c_{1y}}}{\sqrt{c_{3x}}\sqrt{c_{3y}}} \left[z_{1}^{3} m_{1}^{2} + P_{a \to gb}(z_{1}) \left(\mathcal{A}_{+} + \mathcal{B} \cos(2\phi_{1}) \right) \right] \right\}, \quad (3.29a)$$

$$A_{1} = 1 + \frac{q_{1}^{2} P_{a \to gb}(z_{1}) + z_{1}^{3} m_{1}^{2}}{q_{1}^{2} \omega_{a} P_{a \to bg}^{M}(z_{1}, \theta_{1})} 2 \operatorname{Re} i \left\{ \int_{0}^{L} dt_{1} e^{-i\frac{z_{1}^{2}m_{1}^{2}}{2\omega_{a}}(L - t_{1})} e^{-i\frac{q_{1}^{2}}{2\omega_{a}} \left(\frac{\cos^{2} \phi_{1}}{c_{2x}} + \frac{\sin^{2} \phi_{1}}{c_{2y}} \right)} \frac{\sqrt{c_{1x}}}{\sqrt{c_{2x}}} \right. \\
\times \frac{\sqrt{c_{1y}}}{\sqrt{c_{2y}}} \left[\mathcal{D}_{+} + \mathcal{D}_{-} \cos(2\phi_{1}) \right] - \left(\frac{Q_{a}^{2} - m_{1}^{2}}{2p_{a}^{+}} \right) \int_{0}^{L} dt_{1} \int_{t_{1}}^{L} d\bar{t}_{1} e^{-i\frac{z_{1}^{2}m_{1}^{2}}{2\omega_{a}}\Delta t} \\
\times e^{i\frac{q_{1}^{2}}{2\omega_{a}} \left(\frac{\cos^{2} \phi_{1}}{c_{3x}} + \frac{\sin^{2} \phi_{1}}{c_{3y}} \right)} \frac{\sqrt{c_{1x}}\sqrt{c_{1y}}}{\sqrt{c_{3x}}\sqrt{c_{3y}}} \left[\mathcal{C}_{+} + \mathcal{A}_{-} \cos(2\phi_{1}) + \mathcal{C}_{-} \cos(4\phi_{1}) \right] \right\}, \quad (3.29b)$$

$$A_{2} = -\frac{q_{1}^{2} P_{a \to gb}(z_{1}) + z_{1}^{3} m_{1}^{2}}{q_{1}^{2} \omega_{a}} 2 \operatorname{Re} i \left\{ \int_{0}^{L} dt_{1} e^{-i\frac{z_{1}^{2}m_{1}^{2}}{2\omega_{a}}(L - t_{1})} e^{-i\frac{q_{1}^{2}}{2\omega_{a}} \left(\frac{\cos^{2} \phi_{1}}{c_{2x}} + \frac{\sin^{2} \phi_{1}}{c_{2y}} \right)} \frac{\sqrt{c_{1x}}}{\sqrt{c_{2x}}} \right. \\
\times \frac{\sqrt{c_{1y}}}{\sqrt{c_{2x}}} \mathcal{D}_{-} \sin(2\phi_{1}) - \left(\frac{Q_{a}^{2} - m_{1}^{2}}{2p_{a}^{+}} \right) \int_{0}^{L} dt_{1} \int_{t_{1}}^{L} d\bar{t}_{1} e^{-i\frac{z_{1}^{2}m_{1}^{2}}{2\omega_{a}} \Delta t} e^{i\frac{q_{1}^{2}}{2\omega_{a}} \left(\frac{\cos^{2} \phi_{1}}{c_{2x}} + \frac{\sin^{2} \phi_{1}}{c_{2y}} \right)} \\
\times \frac{\sqrt{c_{1x}}}{\sqrt{c_{2y}}} \mathcal{D}_{-} \sin(2\phi_{1}) - \left(\frac{Q_{a}^{2} - m_{1}^{2}}{2p_{a}^{+}} \right) \int_{0}^{L} dt_{1} \int_{t_{1}}^{L} d\bar{t}_{1} e^{-i\frac{z_{1}^{2}m_{1}^{2$$

Finally, the complex c-functions, defined as

$$c_{1i} = \frac{\Omega_i}{2i\sin\Omega_i\Delta t}, \qquad (3.30a)$$

$$c_{2i} = \frac{\Omega_i}{\tan \Omega_i \Delta t} \,, \tag{3.30b}$$

$$c_{3i} = (L - \bar{t}_1) \left(-i \frac{\hat{q}_i f_{a \to bg}(z_1)}{4\omega_a} \right) - c_{2i},$$
 (3.30c)

encode the medium anisotropy and enter into the remaining functions

$$\mathcal{A}_{\pm} = 2\omega_a \left(c_{1x} \pm c_{1y} + \frac{c_{1x}c_{2x}}{c_{3x}} \pm \frac{c_{1y}c_{2y}}{c_{3y}} \right) + i\mathbf{q}_1^2 \left(\frac{c_{1x}c_{2x}}{c_{3x}^2} \pm \frac{c_{1y}c_{2y}}{c_{3y}^2} \right) , \qquad (3.31a)$$

$$\mathcal{B} = i\mathbf{q}_1^2 \left(\frac{c_{1x}c_{2x}}{c_{3x}^2} - \frac{c_{1y}c_{2y}}{c_{3y}^2} \right), \tag{3.31b}$$

$$C_{\pm} = \frac{i\mathbf{q}_1^2}{2} \left(\frac{c_{1x}}{c_{3x}} \pm \frac{c_{1y}}{c_{3y}} \right) \left(\frac{c_{2x}}{c_{3x}} \pm \frac{c_{2y}}{c_{3y}} \right) , \tag{3.31c}$$

$$\mathcal{D}_{\pm} = q_1^2 \left(\frac{c_{1x}}{c_{2x}} \pm \frac{c_{1y}}{c_{2y}} \right). \tag{3.31d}$$

Eqs.(3.27)-(3.31) are the main result of this paper. A few comments are in order before presenting the numerical calculation of this cross-section. First, as a consequence of assuming only the $a \to b g$ splitting to be modified by the medium, the A_1, A_2 and F_{med} auxiliary functions solely depend on the first branching kinematics $(p_a^+, m_1, \theta_1, z_1, \phi_1)$ and on the medium parameters $(L, \hat{q}_x, \hat{q}_y)$. Recovering the vacuum limit, effectively amounts to taking $1 + F_{\text{med}} \to 1, A_1 \to 1, A_2 \to 0$. The existence of odd parity harmonics in ψ_{12} and ϕ_1 , i.e., $\sin(2\psi_{12})$, $\sin(2\phi_1)$ and $\sin(4\phi_1)$, is directly related, under our assumptions, to the medium anisotropy, as previously argued. Note that, in the context of the $1 \to 2$ cross-section in anisotropic media, the odd parity harmonics in ϕ_1 show up only when final-state spin dependence is taken into account [61]. Regarding the direction of anisotropy, we observe that if one inverts it (i.e. $\hat{q}_x \leftrightarrow \hat{q}_y$), then the resulting ϕ_1 distribution is the same as if one transforms it under $\phi_1 \to \phi_1 + \pi/2$. To see this, note that upon switching $\hat{q}_x \leftrightarrow \hat{q}_y$, the coefficients A_- , B, D_- gain a minus sign, while the remaining stay unchanged. All three coefficients are attached to an even harmonic $(\cos(2\phi_1))$ and $\sin(2\phi_1)$, which gains a minus sign under $\phi_1 \to \phi_1 + \pi/2$, canceling the sign from the coefficient. The ϕ_1 dependent phase is trivially invariant under these two simultaneous transformations.

Isotropic medium Setting $\hat{q}_x = \hat{q}_y$ in Eqs. (3.27)-(3.31) leads to a vanishing phase-shift $\phi_{\text{med}} = 0$ together with $A_2 = 0$, i.e., $a_{\text{med}} = aA_1/(1+F_{\text{med}})$. The auxiliary functions reduce to

$$F_{\text{med}} \stackrel{=}{\underset{\hat{q}_{x} = \hat{q}_{y}}{=}} \frac{1}{\omega_{a} P_{a \to bg}^{M}(z_{1}, \theta_{1})} 2 \operatorname{Re} i \left\{ \int_{0}^{L} dt_{1} e^{-i\frac{z_{1}^{2} m_{1}^{2}}{2\omega_{a}}(L - t_{1})} e^{-i\frac{q_{1}^{2}}{2\omega_{a} c_{2}}} \frac{c_{1}}{c_{2}} \left[z_{1}^{3} m_{1}^{2} + P_{a \to gb}(z_{1}) \mathcal{D}_{+} \right] - \left(\frac{Q_{a}^{2} - m_{1}^{2}}{2p_{a}^{+}} \right) \int_{0}^{L} dt_{1} \int_{t_{1}}^{L} d\bar{t}_{1} e^{-i\frac{z_{1}^{2} m_{1}^{2}}{2\omega_{a}} \Delta t} e^{i\frac{q_{1}^{2}}{2\omega_{a} c_{3}}} \frac{c_{1}}{c_{3}} \left[z_{1}^{3} m_{1}^{2} + P_{a \to gb}(z_{1}) \mathcal{A}_{+} \right] \right\},$$

$$A_{1} \stackrel{=}{\underset{\hat{q}_{x} = \hat{q}_{y}}{=}} 1 + \frac{q_{1}^{2} P_{a \to gb}(z_{1}) + z_{1}^{3} m_{1}^{2}}{q_{1}^{2} \omega_{a} P_{a \to bg}^{M}(z_{1}, \theta_{1})} 2 \operatorname{Re} i \left\{ \int_{0}^{L} dt_{1} e^{-i\frac{z_{1}^{2} m_{1}^{2}}{2\omega_{a}}(L - t_{1})} e^{-i\frac{q_{1}^{2}}{2\omega_{a} c_{2}}} \frac{c_{1}}{c_{2}} \mathcal{D}_{-} - \left(\frac{Q_{a}^{2} - m_{1}^{2}}{2p_{a}^{+}} \right) \int_{0}^{L} dt_{1} \int_{t_{1}}^{L} d\bar{t}_{1} e^{-i\frac{z_{1}^{2} m_{1}^{2}}{2\omega_{a}} \Delta t} e^{i\frac{q_{1}^{2}}{2\omega_{a} c_{3}}} \frac{c_{1}}{c_{3}} \mathcal{C}_{+} \right\}.$$

$$(3.32b)$$

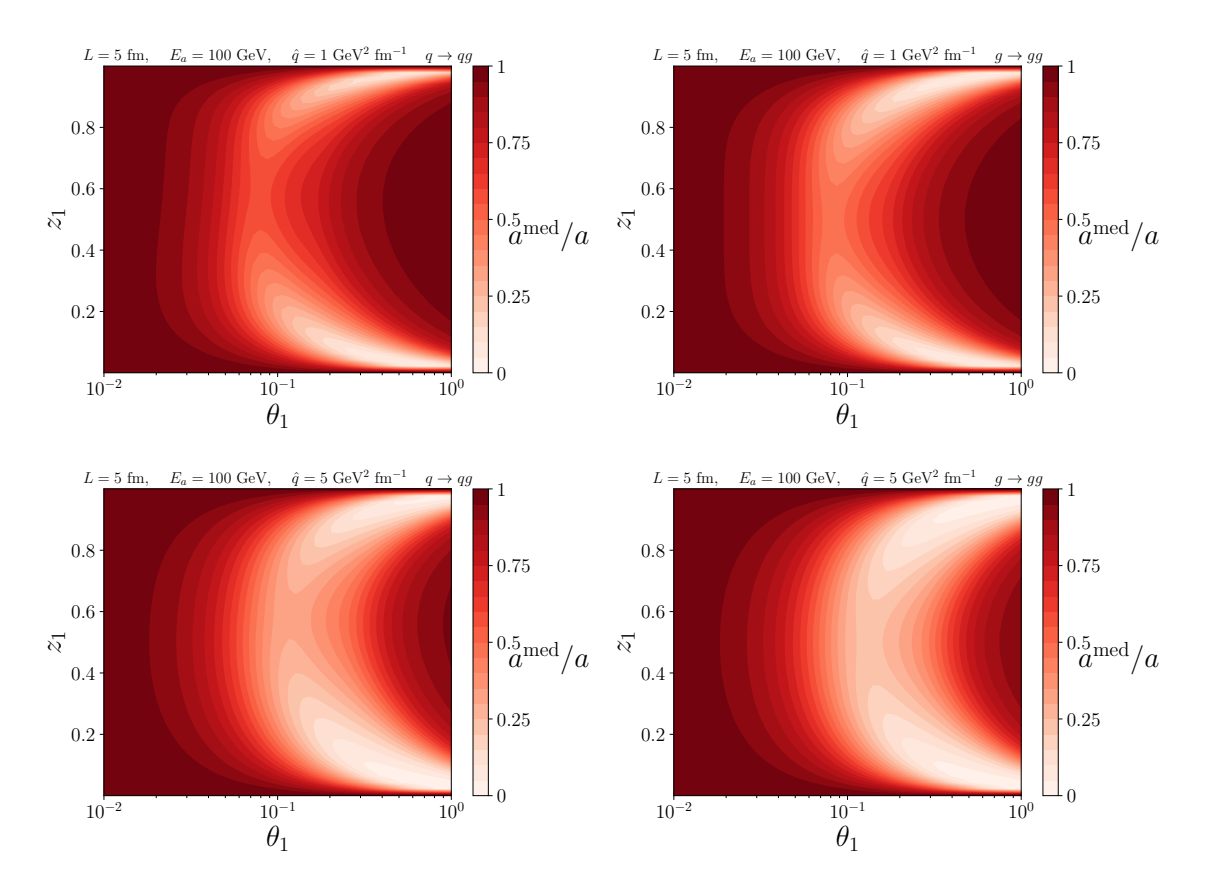


Figure 2: Ratio between the the spin-correlations modulation amplitude in the medium and in vacuum a_{med}/a as a function of the first splitting's kinematics z_1 and θ_1 . The upper panels correspond to the first splitting being $q \to qg$ and the lower ones to $g \to gg$. The medium is isotropic and we plot $\hat{q} = 1 \text{ GeV}^2/\text{fm}$ (upper panels) and 5 GeV²/fm (lower panels).

4 Numerical results

We now numerically evaluate Eq. (3.27), and study the impact of medium modifications on the spin correlations modulation's amplitude a_{med} and their phase shift ϕ_{med} , as well as the total cross-section as a function of the azimuthal angles between planes ψ_{12} . This is done for both an isotropic (Sec. 4.1) and an anisotropic medium (Sec. 4.2) with a fixed medium length of L=5 fm. Similarly to the vacuum results in Sec. 2.2, we take the first splitting to be massless ($m_1=0$) and fix its energy to $E_a=100$ GeV. We emphasize that the second splitting's kinematics (z_2,θ_2) only affects the vacuum piece in Eq. (3.27). Finally, as mentioned above, we do not provide numerical results for F_{med} , since this has been addressed multiple times in the literature (see e.g. [84, 92]).

4.1 Isotropic medium

In Fig. 2, we show the medium-induced modification on the spin-correlations signal, a_{med}/a , as a function of the first splitting's kinematics (z_1, θ_1) and for two values of \hat{q} : $\hat{q} = 1$

GeV²/fm (upper panels) and $\hat{q}=5$ GeV²/fm (lower panels). The left panels correspond to the first splitting being $q\to qg$ and the right panels to $g\to gg$. The $a_{\rm med}/a$ ratio is independent of the second splitting kinematics. The first observation to make is that medium interactions suppress the strength of spin correlations in the bulk of phase-space. Namely, $a_{\rm med}/a$ remains ≤ 1 and, when increasing \hat{q} , the phase space band where this modulation suppression is significant gets wider and, for most of phase space, stronger. In particular phase-space regions, it is even possible that the medium completely washes out the spin correlations effect. Medium effects only vanish for very collinear splittings, $\theta_1 \lesssim 10^{-2}$. The (z_1,θ_1) -dependence of the suppression can be traced back to the formation time of the first splitting given by $\tau_1^{-1} \sim z_1(1-z_1)E_a\theta_1^2$. Then, for $\tau_1 > L$ or $\tau_1 \ll L$ the effect becomes negligible, as expected. Finally, when comparing both channels, we observe that the most significant difference occurs at $z_1 \gtrsim 0.5$. In turn, for $z_1 \ll 1$ no channel-dependence in $a_{\rm med}/a$ is observed since, in this limit, $P_{gq}(z_1) \approx P_{gg}(z_1) \approx 2/z_1$ and the same equality holds for the process-dependent functions in the medium modification in Eq. (3.26).

Next, we evaluate the in-medium cross section stripped off both the vacuum cross-section and the $(1 + F_{\text{med}})$ factor, i.e., we study

$$\mathcal{P}(z_1, \theta_1, z_2, \theta_2, \psi_{12}) \equiv 1 + a_{\text{med}} \cos(2\psi_{12}), \tag{4.1}$$

as a function of ψ_{12} in Fig. 3. We pick (z_1, θ_1) values for which medium modifications are strongest in Fig. 2. The value of $z_2 = 0.5$ is also chosen so as to maximize the azimuthal modulations, see Fig. 1. Finally, we fix $\theta_2 = 0.05 < \theta_1$ to stay within the strongly-ordered approximation. Let us first discuss the vacuum results (black lines). As has been observed in the literature, $g \to gg$ and $g \to q\bar{q}$ splittings feature a correlation with opposite signs. Namely, for $q \to qgg$ splittings (left panels) \mathcal{P} is largest when the two splittings are in the same plane $(\psi_{12}=0)$, while for $g\to q\bar{q}$ (right panels) the spin correlations are largest when the splitting planes are perpendicular. In the massless case, such a modulation is much more pronounced in the $g \to q\bar{q}$ than for $g \to gg$ branchings, see for instance Refs. [22, 25]. However, when considering quarks to be massive, in particular setting $m_2 = m_c$, we get an almost negligible modulation for the explored phase-space points. This is because for the chosen kinematics $\theta_{m,2} \approx 5$, i.e., the splitting occurs deep inside the dead cone. This weak modulation of \mathcal{P} is consistent with the evolution of a with $\theta_{m,2}$ as displayed in Fig. 1. As for the medium results (coloured curves), we find the modulation to be suppressed in agreement with Fig. 2. Further, the evolution of \mathcal{P} with \hat{q} depends on the phase-space point under consideration. For instance, when considering moderately large opening angles such as $\theta = 0.3$ (bottom panels), there is a monotonic trend - larger \hat{q} implies a larger suppression of the modulation. For $\theta = 0.15$ (top panels), however, the trend is non-trivial - for $\hat{q} \sim 1$ GeV²/fm we see a turning point for which the previous trend is reversed. More concretely, for $\hat{q} = 5 \text{ GeV}^2/\text{fm}$ the modulation is less suppressed than for $\hat{q} = 1 \text{ GeV}^2/\text{fm}$. This can be traced back to Fig. 2, where an increase in \hat{q} is not only responsible for a widening of the band where suppression is significant, but also for a slight shift of the band's boundary. Therefore, we conclude that the angular modulation in the medium is always weaker than

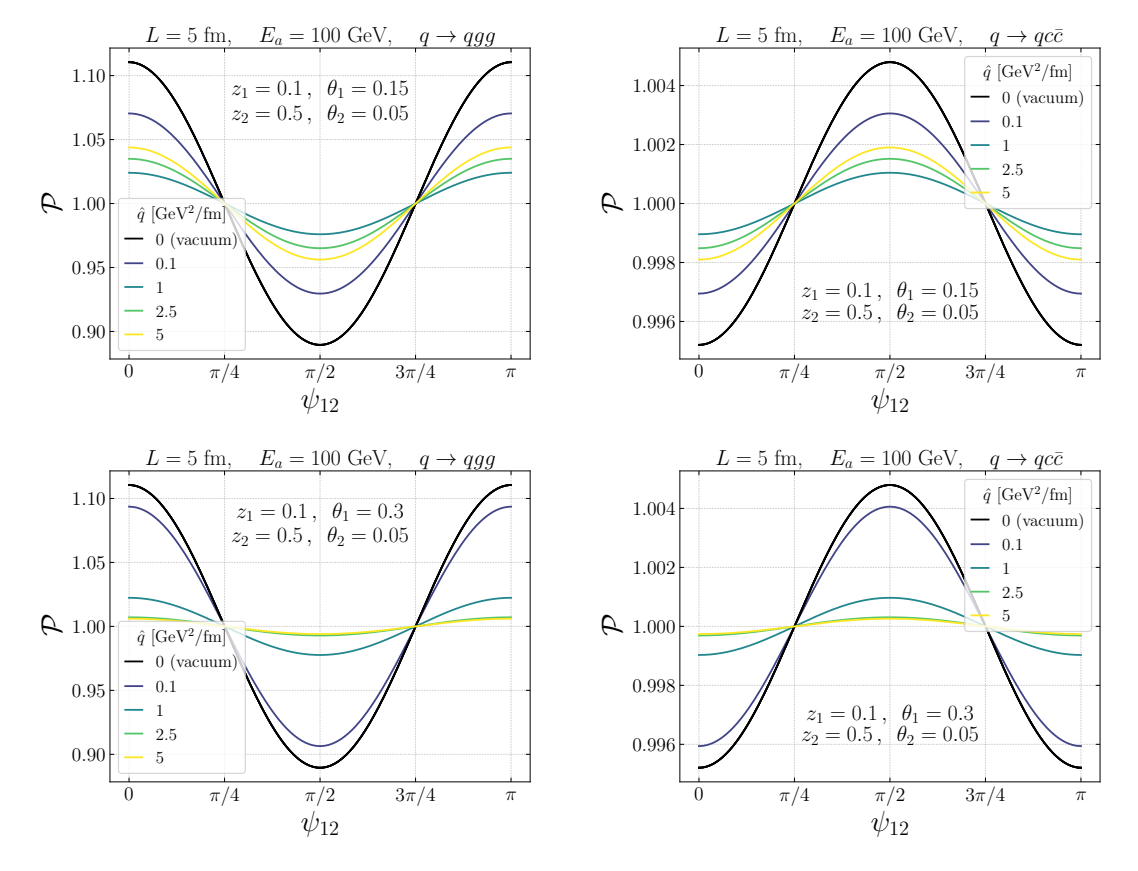


Figure 3: Evolution of the angular modulation in Eq. (4.1) with \hat{q} as a function of ψ_{12} for $\theta_1 = 0.15$ (top panels) and $\theta_1 = 0.3$ (bottom panels). The remaining kinematic variables are fixed to $z_1 = 0.1$, $z_2 = 0.5$ and $\theta_2 = 0.05$. The left panels correspond to $q \to qg \to qgg$ and the right panels to $q \to qg \to qc\bar{c}$. Note that for a massless second splitting (left panels) there is no dependence on θ_2 .

in vacuum and its magnitude depends both on the medium properties and the splitting kinematics.

4.2 Anisotropic medium

We now discuss the case of an anisotropic medium fixing $\hat{q}^{\rm av} = \frac{1}{2}(\hat{q}_x + \hat{q}_y) = 2.5 \text{ GeV}^2/\text{fm}$ and the anisotropy ratio to $\hat{q}_y/\hat{q}_x = 5$. The medium length is fixed to L = 5 fm. Since the dependence on the first channel has been analyzed in the previous section, see Figs. 2,3, we focus on a single process: $q \to qg \to qgg$. The results are presented as a function of the first splitting's kinematics (z_1, θ_1, ϕ_1) with fixed parent's energy $E_a = 100 \text{ GeV}$.

In Fig. 4 we plot the ratio $a_{\rm med}/a_{\rm med}^{\rm iso}$ in the (z_1, θ_1) -plane. This quantity measures the anisotropy-induced modifications on the amplitude of the spin correlations signal. First, we notice that $a_{\rm med}/a_{\rm med}^{\rm iso}$ deviates from unity in a band of phase space which roughly coincides with the one in Fig. 2. As discussed, the shape of this band is controlled by the hierarchy between formation time τ_1 and medium length L. Depending on the azimuthal angle ϕ_1 ,

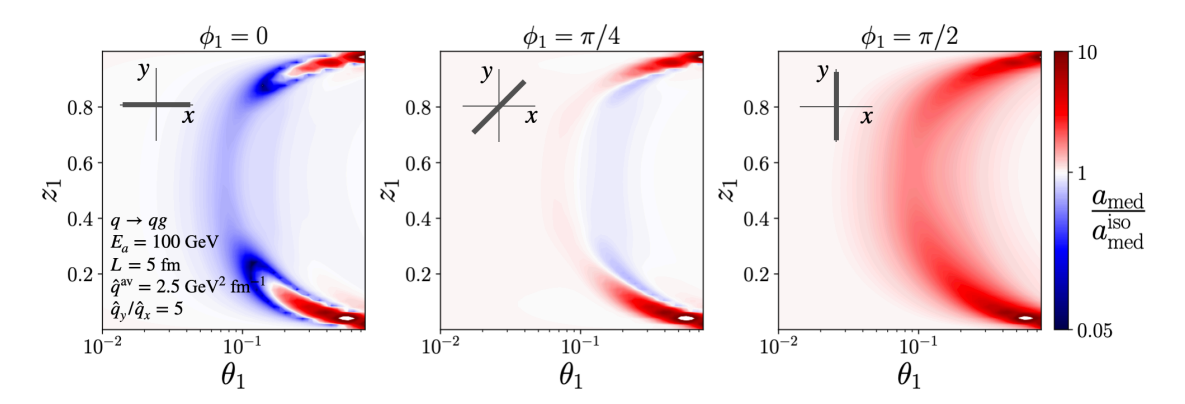


Figure 4: Modulation amplitude a_{med} for an anisotropic medium, divided by the isotropic result with $\hat{q} = \hat{q}^{\text{av}}$ (upper panels) as a function of the first splitting's kinematics z_1 and θ_1 , for the process $q \to qg$. The three columns correspond to three different azimuthal orientations of first splitting's plane: $\phi_1 = 0$, $\pi/4$, $\pi/2$.

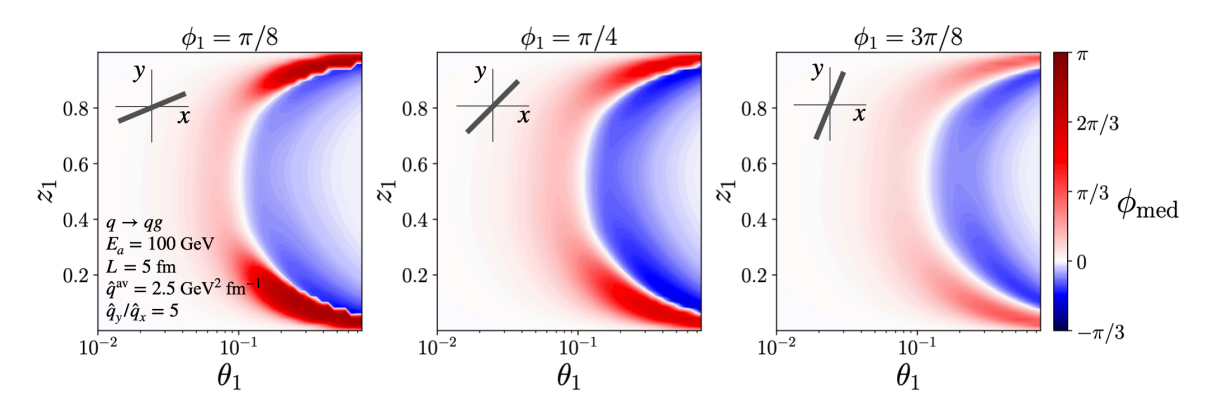
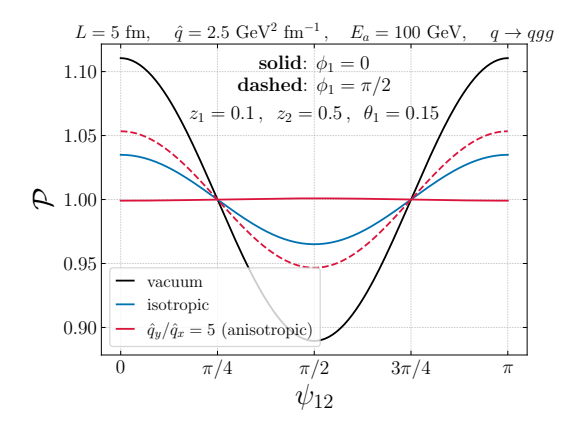


Figure 5: Same as Fig. 4 but for the phase shift ϕ_{med} . The values of ϕ_1 differ with respect to Fig. 4 since $\phi_{\text{med}} = 0$ for $\phi_1 = 0$, $\pi/2$. Here we choose $\phi_1 = \pi/8$, $\pi/4$, $3\pi/8$.

 $a_{\rm med}$ is enhanced (red) or suppressed (blue) in the bulk of phase space with respect to the isotropic case $a_{\rm med}^{\rm iso}$. In particular, for splitting planes orthogonal to the maximal anisotropy direction ($\phi_1 = 0$), one gets mostly a suppression, while for splitting planes aligned with this direction ($\phi_1 = \pi/2$) one gets an enhancement. Interestingly, for $\phi_1 = \pi/4$ one gets a very weak anisotropy-induced modification, which gets significant only for asymmetric, wide angle splittings.

As discussed throughout the calculation presented in Sec. 3, medium anisotropies lead to a unique signature on the spin correlations signal in terms of a phase-shift $\cos(2\psi_{12}) \rightarrow \cos(2\psi_{12} + \phi_{\rm med})$, with $\phi_{\rm med}$ defined in Eq. (3.28b). We show this phase-shift in Fig. 5 as a function of (z_1, θ_1, ϕ_1) . Since $\phi_{\rm med}$ vanishes exactly for $\phi_1 = 0$, $\pi/2$ (see Eq. (3.29)) we choose a different set of ϕ_1 values with respect to Fig. 4. We find that the phase-shift is more pronounced for splitting planes close-to-orthogonal to the maximal anisotropy direction $\phi_1 = \pi/8$. In fact, for specific regions of phase-space, e.g. $\theta_1 > 0.1$ and $z_1 < 0.2$, we obtain $\phi_{\rm med} \approx \pi$ resulting in a sign-change in the azimuthal correlations. Finally, as



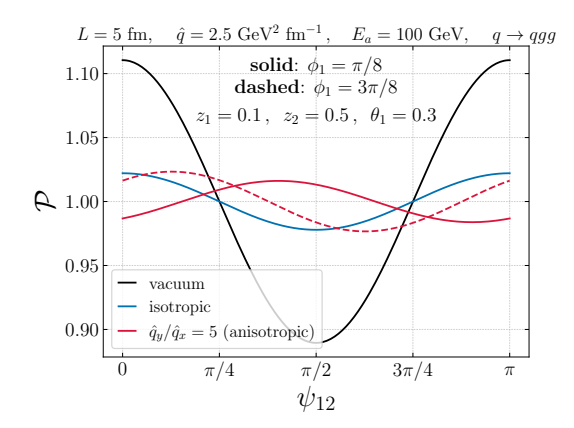


Figure 6: Angular modulation in Eq. (4.1) as a function of ψ_{12} for vacuum (black), isotropic medium (blue) and anisotropic medium (red). The process is fixed to be $q \to qg \to qgg$, so there is no dependence on θ_2 . The energy fractions are fixed to $z_1 = 0.1$ and $z_2 = 0.5$, while $\theta_1 = 0.15$ on the left panel and $\theta_1 = 0.3$ on the right panel. The solid and dashed curves correspond to the first splitting's plane being more aligned with the x and y axis, respectively. In the left plot the medium anisotropy causes only a modulation change, while on the right one it induces only a phase-shift.

one increasingly aligns the splitting plane with the maximal anisotropy ($\phi_1 = 3\pi/8$), ϕ_{med} gradually takes smaller values.

To conclude, we now evaluate the in-medium modification to the cross-section, excluding the $(1 + F_{\text{med}})$ factor:

$$\mathcal{P}(z_1, \theta_1, \phi_1, z_2, \psi_{12}) \equiv 1 + a_{\text{med}} \cos(\psi_{12} + \phi_{\text{med}}). \tag{4.2}$$

Similarly to Fig. 3, we fix the energy fractions to $z_1 = 0.1$ and $z_2 = 0.5$ and choose $\theta_1 = 0.15$ (left panel) and $\theta_1 = 0.3$ (right panel). Since we only focus on the result for a massless second splitting \mathcal{P} does not depend on θ_2 . We plot Eq. (4.2) as a function of ψ_{12} in Fig. 6 for vacuum (black curve), isotropic medium (blue curve) and anisotropic medium with $\hat{q}_y/\hat{q}_x = 5$ (red curves). The solid curve corresponds to the first splitting's plane close to (right panel, $\phi_1 = \pi/8$) or exactly (left panel, $\phi_1 = 0$) orthogonal with maximum anisotropy direction, while the dashed curve corresponds to the first splitting's plane close to (right panel, $\phi_1 = 3\pi/8$) or exactly (left panel, $\phi_1 = \pi/2$) aligned with this direction. The left panel showcases the impact of medium anisotropies on the spin modulation signal purely at the magnitude (a_{med}) level since for $\phi_1 = 0$, $\pi/2$ one has $\phi_{\text{med}} = 0$. For $\phi_1 = 0$ (solid) we observe $\mathcal{P}=1$ or, equivalently, $a_{\text{med}}=1$ in Eq. (4.2), while for $\phi_1=\pi/2$ (dashed) there is a modulation enhancement with respect to the isotropic case. Thus, for certain regions of phase space, anisotropy can fully wash out azimuthal correlations even if they're present for the same region in the case of an isotropic medium. The right panel highlights instead the phase-shift in \mathcal{P} since for this choice of (z_1, θ_1, ϕ_1) the value of $a_{\text{med}}/a_{\text{med}}^{\text{iso}}$ remains close to 1 as can be seen by comparing the blue line with the red, dashed line in the right panel of Fig. 6. For $\phi_1 = \pi/8$ we observe that the anisotropic result for \mathcal{P} is shifted almost 90

degrees with respect to the vacuum and isotropic results ($\phi_{\text{med}} \approx \pi$), in agreement with the findings presented in Fig. 5. We discuss some of the phenomenological challenges related to measuring this phase-shift in the next section.

5 Conclusions

Quantum mechanical interferences driven by colour and spin degrees of freedom are known to break the independent emission picture of QCD radiation. Modifications to the colour interference pattern in the context of jets in heavy-ion collisions have been studied in a series of papers [63–75]. In this work, we have initiated the study of collinear spin correlations in QCD jets that propagate through a quark-gluon plasma. To that end, we have computed the fully differential cross-section to produce a nearly on-shell gluon inside the QGP $(a \to b g)$ and its subsequent branching outside of the medium $(g \to c d)$. The calculation includes mass effects and is performed in the strongly ordered quasi-collinear limit. The main result of this paper is the medium-modified cross section for the process $a \rightarrow b g \rightarrow b c d$ given in Eq. (3.27). Besides the well-known modification of the total rate of emissions encoded in the $F_{\rm med}$ factor, we observe some new striking effects. In vacuum, the polarisation of the intermediate gluon induces an azimuthal correlation between the production and the decay planes. In a dense medium, under our approximations, we find that both the amplitude of this modulation (a_{med}) and its phase (ϕ_{med}) change. These modifications have a non-trivial parametric dependence on the kinematics and partonic flavour of the first splitting as well as on the medium properties. For instance, a_{med} is always smaller than the vacuum baseline but the magnitude of this depletion depends on the channel under consideration, the phase-space point as well as on the medium density, see Figs. 2.4. For specific regions of phase space, the medium can completely suppress the azimuthal modulation. The phase-shift, $\phi_{\rm med}$, only appears when considering anisotropic media since they introduce a preferred direction to which the spin correlation couples. Remarkably, we have shown that for certain phase-space points the medium leads to a 90 degree shift with respect to the vacuum modulation.

There are several caveats when trying to translate the findings of this exploratory, theory study to a realistic measurement at the LHC. Some of these caveats are already present in the proton-proton case. In particular, the observable we have studied, namely the ψ_{12} -distribution, was first proposed in Refs. [22, 25]. There, it was shown that the size of the modulation in a full parton shower decreases with respect to the fixed-order calculation at $\mathcal{O}(\alpha_s^2)$. This is due to two effects: (i) the different sign in the modulation featured by $g \to gg$ and $g \to q\bar{q}$ splittings and (ii) the presence of other branchings not mediated by gluons. These two effects result into the overall spin effect mostly canceling out when considering inclusive jets, as observed in preliminary data from the CMS collaboration [102]. In the medium case, the phase difference between $g \to gg$ and $g \to q\bar{q}$ splittings in the ψ_{12} -distribution competes with the anisotropy-induced phase-shift $\phi_{\rm med}$ that we have studied in Figs. 5 and 6. A possible way out, that has been pursued in the CMS analysis, is to apply heavy-flavour tagging techniques to isolate $g \to q\bar{q}$ splittings and thus obtain a cleaner spin-correlation signal. Such measurement in the heavy-ion case is apriori statistics limited but

it remains to be studied whether it could become feasible in the high-luminosity phase of the LHC [103]. Other proposals to experimentally access spin-dependent quenching effects or medium anisotropies have been presented in Refs. [55, 61, 62, 104].

From a theoretical perspective, there are at least three directions that we would like to pursue to extend the present calculation. The most pressing one, although not straightforward, is to explore the case in which the second splitting takes place inside the medium. A complete calculation of the $1 \to 3$ matrix-element including multiple scatterings with the medium is really challenging. As an intermediate step, one could think of using the $1 \to 3$ results in the collinear limit presented in Ref. [76] where only one scattering between the propagating parton and the medium constituents was considered. Another aspect is how to iterate the calculation that we have presented for multiple branchings in the context of the cascade approximation [76, 105]. In other words, it would be very interesting to formulate the medium analog of the Collins-Knowles algorithm [18, 19]. Finally, we look forward to studying the imprint of medium-induced spin flips on azimuthal correlations between splittings by including helicity-dependent terms in the medium averages as was done in Ref. [106].

The calculation presented in this paper has revealed new qualitative effects in the azimuthal structure of jets in heavy-ion collisions. These results represent a clear step forward in our understanding of in-medium jet physics and we look forward to investigate further into their phenomenological implications in future works.

Acknowledgments

We thank Melissa van Beekveld for insightful discussions on the role of mass effects in spin correlations and João Barata for comments on the manuscript. J.M.S. has been supported by MCIN/AEI (10.13039/501100011033) and ERDF (grant PID2022-139466NB-C21) and by Consejería de Universidad, Investigación e Innovación, Gobierno de España and Unión Europea – NextGenerationEU under grant AST22 6.5. ASO is supported by the Ramón y Cajal program under grant RYC2022-037846-I and from ERDF (grant PID2024-161668NB-100).

A Calculation details

A.1 Kinematics and phase-space parametrization

In the main text we consider any $1 \to 3$ process such that $a \to bg \to bcd$. We first introduce the light-cone energy fractions z_i and the relative transverse momentum of each, $1 \to 2$ splitting

$$z_1 = p_g^+/p_a^+, \quad \boldsymbol{q}_1 = (1 - z_1)\boldsymbol{p}_g - z_1\boldsymbol{p}_b$$
 (A.1a)

$$z_2 = p_c^+/p_g^+, \quad \boldsymbol{q}_2 = (1 - z_2)\boldsymbol{p}_c - z_2\boldsymbol{p}_d$$
 (A.1b)

where we denote $\mathbf{p}_g = \mathbf{p}_c + \mathbf{p}_d$ and the total transverse momentum is $\mathbf{p}_a = \mathbf{p}_b + \mathbf{p}_c + \mathbf{p}_d$. Physically, z_1 is the energy fraction of the intermediate gluon, and z_2 is the energy fraction of the final-state particle with momentum p_c . It's also convenient to define

$$\omega_a = z_1 (1 - z_1) p_a^+,$$
 (A.2a)

$$\omega_a = z_2 (1 - z_2) p_a^+$$
 (A.2b)

We wish to make the change of coordinates $\{p_a, q_1, q_2\} \to \{p_a, \theta_1, \theta_2, \phi_1, \psi_{12}\}$, the definitions of which will become clear in the following text. It is useful to first invert the relations for the transverse momenta in Eq. (A.1)

$$\boldsymbol{p}_b = (1 - z_1)\boldsymbol{p}_a - \boldsymbol{q}_1, \tag{A.3a}$$

$$\mathbf{p}_c = z_1(1 - z_2)\mathbf{p}_a + (1 - z_2)\mathbf{q}_1 - \mathbf{q}_2,$$
 (A.3b)

$$\boldsymbol{p}_d = z_1 z_2 \boldsymbol{p}_a + z_2 \boldsymbol{q}_1 + \boldsymbol{q}_2 \,. \tag{A.3c}$$

and to write the z-component of each momentum in terms of energy and transverse momentum i.e. $p_{iz} = \sqrt{E_i^2 - p_i^2 - m_i^2}$, such that each cartesian three vector is defined in terms of \boldsymbol{p}_a , \boldsymbol{q}_1 , \boldsymbol{q}_2 and m_i . In what follows we work in the quasi-collinear limit, that is we scale all transverse momenta as $\boldsymbol{p} \to \lambda \boldsymbol{p}$ and masses as $m_i \to \lambda m_i$ and keep the first non-vanishing term in a power series of $\lambda \ll 1$.

Then, defining the opening angles of each splitting through the dot product of appropriate three-vectors one finds

$$\theta_1^2/2 = 1 - \frac{\vec{p}_b \cdot \vec{p}_g}{|\vec{p}_b||\vec{p}_a|} = q_1^2/\omega_a^2 + \mathcal{O}(\lambda^4),$$
 (A.4a)

$$\theta_2^2/2 = 1 - \frac{\vec{p}_c \cdot \vec{p}_d}{|\vec{p}_c||\vec{p}_d|} = q_2^2/\omega_g^2 + \mathcal{O}(\lambda^4).$$
 (A.4b)

These expressions for the splitting opening angles are valid up to terms of order $\mathcal{O}(\lambda^4)$, where λ^4 represents any product of four transverse momenta \boldsymbol{p} and/or masses m_i . To relate the azimuthal angles ϕ_1 and ϕ_2 to the angle between the planes spanned by the splittings, which we denote by ψ_{12} , we start with the definition of this quantity as the angle between the normal vectors to each plane. The normal three-vectors of unit norm are defined as the following cross product

$$\vec{n}_1 = \frac{\vec{p}_a \times \vec{p}_g}{|\vec{p}_a \times \vec{p}_g|}, \quad \vec{n}_2 = \frac{\vec{p}_c \times \vec{p}_d}{|\vec{p}_c \times \vec{p}_d|},$$
 (A.5)

so that $\cos(\psi_{12})$ is defined as

$$\cos(\psi_{12}) = \vec{n}_1 \cdot \vec{n}_2 \,, \tag{A.6}$$

which can now be written as a function of p_a , q_1 , q_2 and m_i exactly as was done for the opening angles, using Eq. (A.3). By keeping only terms up to $\mathcal{O}(\lambda^2)$, where λ^2 is any quadratic product of p and m_i , one arrives at

$$\cos \psi_{12} = \frac{\mathbf{q}_1 \cdot \mathbf{q}_2}{|\mathbf{q}_1| |\mathbf{q}_2|} + \mathcal{O}(\lambda^2) \implies \psi_{12} = \phi_2 - \phi_1. \tag{A.7}$$

By using the relations in Eq. (A.4) together with Eq. (A.7), we can now write the Jacobian for the change of coordinates $\{\boldsymbol{p}_a,\boldsymbol{q}_1,\boldsymbol{q}_2\} \to \{\boldsymbol{p}_a,\theta_1,\theta_2,\phi_1,\psi_{12}\}$

$$d^{2} \boldsymbol{p}_{a} d^{2} \boldsymbol{q}_{1} d^{2} \boldsymbol{q}_{2} = \omega_{a}^{2} \omega_{g}^{2} \theta_{1} \theta_{2} / 4 \left(d^{2} \boldsymbol{p}_{a} d\theta_{1} d\theta_{2} d\phi_{1} d\psi_{12} \right)$$

$$= d^{2} \boldsymbol{p}_{a} d\theta_{1} d\theta_{2} d\phi_{1} d\psi_{12} \frac{z_{1}^{4} (1 - z_{1})^{2} z_{2}^{2} (1 - z_{2})^{2} (p_{a}^{+})^{4} \theta_{1} \theta_{2}}{4}. \tag{A.8}$$

This Jacobian becomes relevant when promoting splitting amplitudes \mathcal{M} to differential cross-sections, by including the appropriate phase-space element, i.e.

$$2p_b^+ 2p_c^+ 2p_d^+ (2\pi)^9 \frac{d\sigma}{dp_b^+ dp_c^+ dp_d^+ d^2 \mathbf{p}_b d^2 \mathbf{p}_c d^2 \mathbf{p}_d} = \frac{1}{2} \sum_{\rho_i, \lambda_i} \mathcal{M} \mathcal{M}^{\dagger}. \tag{A.9}$$

where the sum runs over colours (ρ_i) and spin states (λ_i) . The factor 1/2 accounts for the average over the initial parton spin state that we have denoted λ_a in the main text. Let us rewrite the phase-space element in Eq. (A.9) in terms of the relative transverse momenta q_i and energy fractions z_i

$$2z_1(1-z_1)2z_2(1-z_2)(2\pi)^6 \frac{d\sigma}{d^3\Omega_a dz_1 dz_2 d^2 \mathbf{q}_1 d^2 \mathbf{q}_2} = \frac{1}{2} \sum_{\mathbf{q}_i, \lambda_i} \mathcal{M} \mathcal{M}^{\dagger}, \qquad (A.10)$$

where

$$d^{3}\Omega_{a} = \frac{dp_{a}^{+}}{(2\pi)2p_{a}^{+}} \frac{d^{2}\mathbf{p}_{a}}{(2\pi)^{2}}, \tag{A.11}$$

corresponds to the phase-space element of the total momentum of the system. Then, by using Eqs. (A.8) and (A.10), we can re-write Eq. (A.9) as

$$\frac{16(2\pi)^6}{z_1^3(1-z_1)z_2(1-z_2)\theta_1\theta_2} \frac{d\sigma}{dz_1 dz_2 d\theta_1 d\theta_2 d\phi_1 d\psi_{12}} = \frac{1}{2} \sum_{\rho_i, \lambda_i} \int d^3\Omega_a (p_a^+)^4 \mathcal{M} \mathcal{M}^{\dagger} . \quad (A.12)$$

To keep the notation compact, we define

$$d^6\Omega_{\rm PS} \equiv dz_1 \, dz_2 \, d\theta_1 d\theta_2 d\phi_1 d\psi_{12} \,, \tag{A.13}$$

and express the fully differential cross-section as $d\sigma/d^6\Omega_{\rm PS}$.

A.2 Spin-dependent QCD vertices

Consider the QCD splitting $i(p_0, \lambda_0) \to j(p_1, \lambda_1)k(p_2, \lambda_2)$, where p_i are the particle momenta and $\lambda_i = \pm 1$ are their spin states. The spin-dependent vertices can be directly calculated from the following expressions

$$V_{q \to gq}^{\lambda_0 \lambda_1 \lambda_2}(p_1, p_2) = \bar{u}^{\lambda_2}(p_2) \not \in {}^{*,\lambda_1}(p_1) u^{\lambda_0}(p_0)$$
(A.14a)

$$V_{g \to q\bar{q}}^{\lambda_0 \lambda_1 \lambda_2}(p_1, p_2) = \bar{u}^{\lambda_1}(p_1) \not\in^{\lambda_0}(p_0) v^{\lambda_2}(p_2) , \qquad (A.14b)$$

$$V_{g \to gg}^{\lambda_0 \lambda_1 \lambda_2}(p_1, p_2) = \epsilon_{\alpha}^{\lambda_0}(p_0) \epsilon_{\beta}^{*,\lambda_1}(p_1) \epsilon_{\gamma}^{*,\lambda_2}(p_2) [g^{\alpha\beta}(p_0 + p_1)^{\gamma} - g^{\beta\gamma}(p_1 - p_2)^{\alpha} - g^{\gamma\alpha}(p_0 + p_2)^{\beta}],$$
(A.14c)

where $p_0 = p_1 + p_2$. The states λ_i are defined as twice the spin projection along z for quarks and as the circular polarisation state for gluons. The gluon polarisation vector is defined in light-cone gauge as

$$\epsilon^{+,\lambda}(p) = 0, \quad \epsilon^{-,\lambda}(p) = \frac{\epsilon^{\lambda} \cdot \mathbf{p}}{p^{+}}, \quad \epsilon^{\lambda} = \frac{1}{\sqrt{2}}(1, i\lambda).$$
(A.15)

By using this polarisation vector together with the canonical Dirac spinors, these vertices read (see e.g. [22, 107–109])

$$V_{q\to gq}^{\lambda_0\lambda_1\lambda_2}(z,\boldsymbol{q}) = \frac{2\delta^{\lambda_0\lambda_2}}{z\sqrt{1-z}} (\delta^{\lambda_0,\lambda_1} + (1-z)\delta^{\lambda_0,-\lambda_1})(\boldsymbol{q}\cdot\boldsymbol{\epsilon}^{*,\lambda_1}) - \lambda_0\delta^{\lambda_0,-\lambda_2}\delta^{\lambda_0,\lambda_1}\frac{\sqrt{2}zm}{\sqrt{1-z}},$$
(A.16a)

$$V_{g \to q\bar{q}}^{\lambda_0 \lambda_1 \lambda_2}(z, \boldsymbol{q}) = \frac{2\lambda_1 \delta^{\lambda_1, \lambda_2}}{\sqrt{z(1-z)}} (z\delta^{\lambda_0, \lambda_1} - (1-z)\delta^{\lambda_0, -\lambda_1}) (\boldsymbol{q} \cdot \boldsymbol{\epsilon}^{\lambda_0}) - \delta^{\lambda_1, -\lambda_2} \delta^{\lambda_0, \lambda_1} \frac{\sqrt{2}m}{\sqrt{z(1-z)}},$$
(A.16b)

$$V_{g\to gg}^{\lambda_0\lambda_1\lambda_2}(z,\boldsymbol{q}) = 2\left(\frac{\delta^{\lambda_0,\lambda_1}\delta^{\sigma,\lambda_2}}{1-z} - \delta^{\lambda_1,-\lambda_2}\delta^{\sigma,-\lambda_0} + \frac{\delta^{\lambda_0,\lambda_2}\delta^{\sigma,\lambda_1}}{z}\right)(\boldsymbol{q}\cdot\boldsymbol{\epsilon}^{*,\sigma}), \tag{A.16c}$$

where $z = p_1^+/p_0^+$ corresponds to the energy fraction of particle j in the splitting and $\mathbf{q} = (1-z)\mathbf{p}_1 - z\mathbf{p}_2$. Note that the dot product between the relative transverse momentum and the gluon polarisation vector carries information about the azimuthal angle, since one can write it as

$$\mathbf{q} \cdot \boldsymbol{\epsilon}^{\lambda} = \frac{|\mathbf{q}|}{\sqrt{2}} e^{i\lambda\phi} \,. \tag{A.17}$$

This allows to factor out the azimuthal dependence in each vertex as a single overall phase [22, 25]

$$V^{\lambda_0 \lambda_1 \lambda_2}(z, \mathbf{q}) = \tilde{V}^{\lambda_0 \lambda_1 \lambda_2}(z, |\mathbf{q}|) e^{i(\bar{\lambda}_0 - \bar{\lambda}_1 - \bar{\lambda}_2)\phi}, \qquad (A.18)$$

where $\bar{\lambda}_i = \lambda_i$ if the particle is a gluon and $\bar{\lambda}_i = \pm \lambda_i/2$ if the particle is a quark or antiquark, respectively. In \tilde{V} one replaces $\mathbf{q} \cdot \mathbf{\epsilon} \to |\mathbf{q}|/\sqrt{2}$ in V. This can be readily checked by plugging this phase in Eq. (A.16).

In the main text, we wish to compute the cross-section for the process $a \to b g \to b c d$. At the scattering amplitude level, this involves a sum over the intermediate gluon's polarisations (λ_g) of a product of vertices,

$$\mathcal{A}(\boldsymbol{q}_1, \boldsymbol{q}_2) \equiv \sum_{\lambda_g} V_{g \to cd}^{\lambda_g \lambda_c \lambda_d}(z_2, \boldsymbol{q}_2) V_{a \to bg}^{\lambda_a \lambda_g \lambda_b}(z_1, \boldsymbol{q}_1), \qquad (A.19)$$

while for the squared-matrix element we also need to sum over final state spin states $\lambda_b, \lambda_c, \lambda_d$ and average over the initial state one λ_a . One can verify that, in vacuum, the product of any QCD vertex in Eq. (A.16) and its complex conjugate is polarisation independent when considering a different polarisation for the off-shell gluon in the amplitude

and complex conjugate amplitude, as was stated in Eq. (2.6). For instance, for a $g \to q\bar{q}$ splitting with energy fraction z and transverse momentum q we find

$$\sum_{\lambda_q \lambda_{\bar{q}}} \tilde{V}_{g \to q\bar{q}}^{\lambda_g \lambda_q \lambda_{\bar{q}}}(z, \boldsymbol{q}) \tilde{V}_{g \to q\bar{q}}^{*, \lambda'_g \lambda_q \lambda_{\bar{q}}}(z, \boldsymbol{q}) = \frac{2}{z(1-z)} \left(\delta^{\lambda_g, \lambda'_g}(m_q^2 + \boldsymbol{q}^2 P_{qg}(z)) - \delta^{\lambda_g, -\lambda'_g} 2z(1-z) \boldsymbol{q}^2 \right), \tag{A.20}$$

i.e., the functions attached to both δ tensors are independent of λ_g and λ_g' . This implies, in particular, that there is no $\sin(2\psi_{12})$ modulation due to spin correlations (see Eq. (A.25)). However, if we assume the first splitting $a \to b g$ to happen inside a QCD medium while the gluon splits in vacuum (see Eq. (3.4)), one can show that polarisation dependent terms arise when there is some type of anisotropy in the transverse plane which breaks rotational invariance of the medium. To see this, consider the contribution coming from the term with $\lambda_g \neq \lambda_g'$ in the square of the $a \to b g$ vertex. Due to interactions with the medium, one writes this with different relative transverse momentum in the amplitude (κ) and in the conjugate amplitude (κ) ,

$$\delta^{\lambda_g, -\lambda'_g} \sum_{\lambda_a \lambda_b} V_{a \to gb}^{\lambda_a \lambda_g \lambda_b}(z, \boldsymbol{\kappa}) V_{a \to gb}^{*, \lambda_a \lambda'_g \lambda_b}(z, \bar{\boldsymbol{\kappa}}) e^{i(\lambda_g - \lambda'_g)\phi_2} \propto \delta^{\lambda_g, -\lambda'_g} e^{-i\lambda_g(\phi_{\boldsymbol{\kappa}} + \phi_{\bar{\boldsymbol{\kappa}}} - 2\phi_2)}, \quad (A.21)$$

where $\kappa = |\kappa|(\cos\phi_{\kappa}, \sin\phi_{\kappa})$ and the same for $\bar{\kappa}$, and the angle ϕ_2 is the azimuthal orientation of the final-state plane formed by b and g. If the medium is rotationally invariant the dependence on ϕ_2 in Eq. (A.21) vanishes. Also, the remaining function of κ and $\bar{\kappa}$ against which Eq. (A.21) is integrated depends only on κ^2 , $\bar{\kappa}^2$ and $\phi_{\kappa} - \phi_{\bar{\kappa}}$. Hence, the phase $e^{i\lambda_g(\phi_{\kappa} + \phi_{\bar{\kappa}})}$ can be integrated out to yield a λ_g independent result.

Finally, for all vertices in Eq. (A.16), one can show that the square of Eq. (A.19) entering the product of the amplitude and conjugate amplitude reads

$$\frac{1}{2} \sum_{\lambda_a} \sum_{\lambda_b \lambda_c \lambda_d} \mathcal{A}(\boldsymbol{\kappa}, \boldsymbol{q}_2) \mathcal{A}^{\dagger}(\bar{\boldsymbol{\kappa}}, \boldsymbol{q}_2) = \frac{4(m_2^2 + \boldsymbol{q}_2^2 P_{g \to cd}(z_2))}{z_2 (1 - z_2) z_1 (1 - z_1)} \times \left[z_1^3 m_1^2 + P_{a \to gb}(z_1) \left(\boldsymbol{\kappa} \cdot \bar{\boldsymbol{\kappa}} \right) \right] \\
\mp \frac{4z_2 (1 - z_2) (1 - z_1)}{z_1 (m_2^2 + \boldsymbol{p}_{23}^2 P_{g \to cd}(z_2))} \left((\boldsymbol{q}_2 \cdot \boldsymbol{\kappa}) \left(\boldsymbol{q}_2 \cdot \bar{\boldsymbol{\kappa}} \right) - (\boldsymbol{q}_2 \times \boldsymbol{\kappa})_z \left(\boldsymbol{q}_2 \times \bar{\boldsymbol{\kappa}} \right)_z \right) \right] \tag{A.22}$$

where $(q_2 \times \kappa)_z = q_2^x \kappa^y - q_2^y \kappa^x$, κ and $\bar{\kappa}$ correspond to integration variables in the medium calculation, and all other variables are defined in Eq. (A.1). The channel-dependence of Eq. (A.22) is encoded in the factor \pm which takes into account if the intermediate gluon splits into a $q\bar{q}$ pair (+) or a pair of gluons (-), and in $P_{ji}(z)$ which is the massless splitting function for the process $i \to jk$ stripped of its corresponding colour factor

$$P_{q \to gq}(z) = \frac{1 + (1 - z)^2}{z},$$
 (A.23a)

$$P_{g \to q\bar{q}}(z) = z^2 + (1-z)^2,$$
 (A.23b)

$$P_{g \to gg}(z) = 2\left(\frac{z}{1-z} + \frac{1-z}{z} + z(1-z)\right).$$
 (A.23c)

⁹Note that this reasoning is only valid because we assumed the gluon splits in vacuum. Were this not true, then a dependence on $\psi_{12} = \phi_2 - \phi_1$ would exist for the medium modification. Thus, the integrand could depend on, e.g., $(\phi_{\kappa} - \psi_{12}) + (\phi_{\bar{\kappa}} - \psi_{12})$.

Note that $m_1 = m_a = m_b$ and and $m_2 = m_c = m_d$.

In the vacuum case Eq. (A.22) can be further simplified by setting $\kappa = \bar{\kappa} = q_1$ such that the squared amplitude reads

$$\frac{1}{2} \sum_{\lambda_{a}} \sum_{\lambda_{b} \lambda_{c} \lambda_{d}} \mathcal{A}(\boldsymbol{q}_{1}, \boldsymbol{q}_{2}) \mathcal{A}^{\dagger}(\boldsymbol{q}_{1}, \boldsymbol{q}_{2}) = \frac{4(m_{2}^{2} + \boldsymbol{q}_{2}^{2} P_{g \to cd}(z_{2}))}{z_{2}(1 - z_{2})z_{1}(1 - z_{1})} \times \left[z_{1}^{3} m_{1}^{2} + P_{a \to gb}(z_{1}) \boldsymbol{q}_{1}^{2} + \frac{4z_{2}(1 - z_{2})(1 - z_{1})}{z_{1}(m_{2}^{2} + \boldsymbol{q}_{2}^{2} P_{g \to cd}(z_{2}))} \left((\boldsymbol{q}_{2} \cdot \boldsymbol{q}_{1})^{2} - |\boldsymbol{q}_{2} \times \boldsymbol{q}_{1}|^{2} \right) \right].$$
(A.24)

By using Eq. (A.7), we can re-write the scalar and vector products in terms of the azimuthal angle between the planes spanned by the two splittings:

$$\frac{1}{2} \sum_{\lambda_a} \sum_{\lambda_b \lambda_c \lambda_d} \mathcal{A}(\boldsymbol{q}_1, \boldsymbol{q}_2) \mathcal{A}^{\dagger}(\boldsymbol{q}_1, \boldsymbol{q}_2) = \frac{4(m_2^2 + \boldsymbol{q}_2^2 P_{3g}(z_2))}{z_2(1 - z_2)z_1(1 - z_1)} \times \left[z_1^3 m_1^2 + P_{a \to gb}(z_1) \boldsymbol{q}_1^2 \mp \frac{4z_2(1 - z_2)(1 - z_1) \boldsymbol{q}_1^2 \boldsymbol{q}_2^2}{z_1(m_2^2 + \boldsymbol{p}_{23}^2 P_{3g}(z_2))} \cos(2\psi_{12}) \right], \tag{A.25}$$

This form for the $\cos(2\psi_{12})$ modulation in vacuum for $1 \to 3$ processes with an intermediate gluon is well known in the literature (see e.g. [15, 18, 19, 22, 25, 82]). Processes with no intermediate off-shell gluons (e.g. $q \to qg \to qgg$) do not exhibit such a dependence.

A.3 n-point medium averages in the large- N_c limit

The objects K and Q used in the main text are defined, in the large- N_c limit, as

$$\mathcal{K}_{a \to bg}(\bar{t}_1, \boldsymbol{q}_1; t_1, \boldsymbol{\kappa}) = \int_{\boldsymbol{u}_1, \boldsymbol{u}_2} e^{i\boldsymbol{u}_1 \cdot \boldsymbol{\kappa}} e^{-i\boldsymbol{u}_2 \cdot \boldsymbol{l}} \int_{\boldsymbol{u}_1}^{\boldsymbol{u}_2} \mathcal{D} \boldsymbol{u} \exp \left\{ i \frac{\omega_a}{2} \int_{t_1}^{\bar{t}_1} ds \, \dot{\boldsymbol{u}}^2 \right\} \mathcal{C}_{a \to bg}^{(3)}(\bar{t}_1, t_1; \boldsymbol{u}), \tag{A.26a}$$

$$\mathcal{Q}_{a\to bg}(L, \boldsymbol{q}_1, \boldsymbol{q}_1; \bar{t}_1, \bar{\boldsymbol{\kappa}}, \boldsymbol{l}) = \int_{\boldsymbol{u}_i, \boldsymbol{u}_f, \bar{\boldsymbol{u}}_i, \bar{\boldsymbol{u}}_f} e^{i\boldsymbol{u}_i \cdot \boldsymbol{l}} e^{-i\bar{\boldsymbol{u}}_i \cdot \bar{\boldsymbol{\kappa}}} e^{-i(\boldsymbol{u}_f - \bar{\boldsymbol{u}}_f) \cdot \boldsymbol{q}_1} \\
\times \int_{\boldsymbol{u}_f}^{\boldsymbol{u}_f} \mathcal{D} \boldsymbol{u} \int_{\bar{\boldsymbol{v}}_i}^{\bar{\boldsymbol{u}}_f} \mathcal{D} \bar{\boldsymbol{u}} \exp \left\{ i \frac{\omega_a}{2} \int_{\bar{\boldsymbol{t}}_i}^{L} ds \left(\dot{\boldsymbol{u}}^2 - \dot{\bar{\boldsymbol{u}}}^2 \right) \right\} \mathcal{C}_{a\to bg}^{(4)}(L, \bar{t}_1; \boldsymbol{u}, \bar{\boldsymbol{u}}) . \tag{A.26b}$$

The *n*-point functions $C^{(3)}$ and $C^{(4)}$ are given in terms of dipole and quadrupole objects. For the relevant processes, one can write them as

$$C_{q\to gq}^{(3)}(\bar{t},t;\boldsymbol{u}) = D(\bar{t},t;\boldsymbol{u})D(\bar{t},t;(1-z)\boldsymbol{u}), \qquad (A.27a)$$

$$C_{a \to a q}^{(3)}(\bar{t}, t; \boldsymbol{u}) = D(\bar{t}, t; \boldsymbol{u})D(\bar{t}, t; z\boldsymbol{u})D(\bar{t}, t; (1 - z)\boldsymbol{u}), \tag{A.27b}$$

$$C_{q \to qq}^{(4)}(\bar{t}, t; \boldsymbol{v}, \bar{\boldsymbol{v}}) = Q(\bar{t}, t; \boldsymbol{v}, \bar{\boldsymbol{v}}) D(\bar{t}, t; -(1 - z_1)(\boldsymbol{v} - \bar{\boldsymbol{v}})), \qquad (A.27c)$$

$$C_{g\to gg}^{(4)}(\bar{t},t;\boldsymbol{v},\bar{\boldsymbol{v}}) = Q(\bar{t},t;\boldsymbol{v},\bar{\boldsymbol{v}})D(\bar{t},t;-(1-z_1)(\boldsymbol{v}-\bar{\boldsymbol{v}}))D(\bar{t},t;-z_1(\boldsymbol{v}-\bar{\boldsymbol{v}})), \qquad (A.27d)$$

where $U_i^{jk} = U_F^{jk}(\bar{t}, t; \boldsymbol{r}_i)$ as defined in Eq. (3.8) and the dipole is defined in Eq. (3.20). The quadrupole is defined as $Q(\bar{t}, t; \boldsymbol{v}, \bar{\boldsymbol{v}}) = \frac{1}{N_c} \left\langle \operatorname{Tr} \left(U_1^{\dagger} U_2 U_3^{\dagger} U_4 \right) \right\rangle$, with the relevant differences

of coordinates r_i being defined as

$$\boldsymbol{r}_1 - \boldsymbol{r}_2 = (1 - z_1)(\boldsymbol{v} - \bar{\boldsymbol{v}}), \qquad (A.28a)$$

$$\mathbf{r}_3 - \mathbf{r}_4 = z_1(\mathbf{v} - \bar{\mathbf{v}}), \tag{A.28b}$$

$$\boldsymbol{r}_1 - \boldsymbol{r}_4 = \boldsymbol{v} \,. \tag{A.28c}$$

Keeping this object in its full form results in a quite involved calculation of the $C^{(4)}$ function (see e.g. [84, 92, 95, 100]). As explained in the main text near Eq. (3.19), we simplify it by approximating it as the independent broadening of the two final state partons, which amounts to writing the quadrupole as

$$Q(\bar{t}, t; \boldsymbol{v}, \bar{\boldsymbol{v}}) \approx D(\bar{t}, t; z_1(\boldsymbol{v} - \bar{\boldsymbol{v}}))D(\bar{t}, t; (1 - z_1)(\boldsymbol{v} - \bar{\boldsymbol{v}})) \equiv \mathcal{P}(\bar{t}, t; \boldsymbol{v} - \bar{\boldsymbol{v}}). \tag{A.29}$$

With this approximation, everything is given in terms of dipoles, such that K and Q are simplified to

$$Q_{a\to bg}(L, \boldsymbol{q}_1, \boldsymbol{q}_1; \bar{t}_1, \bar{\boldsymbol{\kappa}}, \boldsymbol{l}) \equiv \delta^2(\boldsymbol{l} - \bar{\boldsymbol{\kappa}}) \int_{\boldsymbol{v}} e^{-i\boldsymbol{v}\cdot(\boldsymbol{q}_1 - \bar{\boldsymbol{\kappa}})} \mathcal{P}_{a\to gb}(L, \bar{t}_1, \boldsymbol{v}), \qquad (A.30a)$$

$$\int_{\boldsymbol{l}} \delta^{2}(\boldsymbol{l} - \bar{\boldsymbol{\kappa}}) \mathcal{K}_{a \to bg}(\bar{t}_{1}, \boldsymbol{l}; t_{1}, \boldsymbol{\kappa}) \equiv \int_{\boldsymbol{u}_{1}, \boldsymbol{u}_{2}} e^{i\boldsymbol{u}_{1} \cdot \boldsymbol{\kappa}} e^{-i\boldsymbol{u}_{2} \cdot \bar{\boldsymbol{\kappa}}} \mathcal{K}_{a \to bg}(\bar{t}_{1}, \boldsymbol{u}_{2}; t_{1}, \boldsymbol{u}_{1}).$$
(A.30b)

References

- A. Bassetto, M. Ciafaloni, and G. Marchesini, Jet Structure and Infrared Sensitive Quantities in Perturbative QCD, Phys. Rept. 100 (1983) 201–272.
- [2] Y. L. Dokshitzer, G. Marchesini, and G. Oriani, Measuring color flows in hard processes: Beyond leading order, Nucl. Phys. B 387 (1992) 675–714.
- [3] J. M. Campbell and E. W. N. Glover, Double unresolved approximations to multiparton scattering amplitudes, Nucl. Phys. B 527 (1998) 264–288, [hep-ph/9710255].
- [4] S. Catani and M. Grazzini, Infrared factorization of tree level QCD amplitudes at the next-to-next-to-leading order and beyond, Nucl. Phys. B **570** (2000) 287–325, [hep-ph/9908523].
- [5] J. M. Campbell et al., Event generators for high-energy physics experiments, SciPost Phys. 16 (2024), no. 5 130, [arXiv:2203.11110].
- [6] Y. L. Dokshitzer, V. S. Fadin, and V. A. Khoze, Coherent Effects in the Perturbative QCD Parton Jets, Phys. Lett. B 115 (1982) 242–246.
- [7] B. R. Webber, A QCD Model for Jet Fragmentation Including Soft Gluon Interference, Nucl. Phys. B 238 (1984) 492–528.
- [8] G. Marchesini and B. R. Webber, Monte Carlo Simulation of General Hard Processes with Coherent QCD Radiation, Nucl. Phys. B 310 (1988) 461–526.
- [9] Y. L. Dokshitzer, V. A. Khoze, S. I. Troian, and A. H. Mueller, QCD Coherence in High-Energy Reactions, Rev. Mod. Phys. 60 (1988) 373.
- [10] G. Gustafson and U. Pettersson, Dipole Formulation of QCD Cascades, Nucl. Phys. B 306 (1988) 746–758.

- [11] Z. Nagy and D. E. Soper, Parton showers with more exact color evolution, Phys. Rev. D 99 (2019), no. 5 054009, [arXiv:1902.02105].
- [12] K. Hamilton, R. Medves, G. P. Salam, L. Scyboz, and G. Soyez, Colour and logarithmic accuracy in final-state parton showers, JHEP 03 (2021), no. 041 041, [arXiv:2011.10054].
- [13] J. R. Forshaw, S. Plätzer, and F. T. González, Fully differential soft gluon evolution at the amplitude level, JHEP 09 (2025) 207, [arXiv:2505.13183].
- [14] A. V. Efremov and O. V. Teryaev, On Spin Effects in Quantum Chromodynamics, Sov. J. Nucl. Phys. 36 (1982) 140.
- [15] M. P. Shatz, Leading Log Approximation for Parton Showers, Nucl. Phys. B 224 (1983) 218–228.
- [16] B. R. Webber, Monte Carlo Simulation of Hard Hadronic Processes, Ann. Rev. Nucl. Part. Sci. 36 (1986) 253–286.
- [17] B. R. Webber, Quantum Correlations in QCD Jets, Phys. Lett. B 193 (1987) 91–94.
- [18] J. C. Collins, Spin Correlations in Monte Carlo Event Generators, Nucl. Phys. B 304 (1988) 794–804.
- [19] I. G. Knowles, Angular Correlations in QCD, Nucl. Phys. B 304 (1988) 767–793.
- [20] I. G. Knowles, Spin Correlations in Parton Parton Scattering, Nucl. Phys. B 310 (1988) 571–588.
- [21] I. G. Knowles, A Linear Algorithm for Calculating Spin Correlations in Hadronic Collisions, Comput. Phys. Commun. 58 (1990) 271–284.
- [22] P. Richardson and S. Webster, Spin Correlations in Parton Shower Simulations, Eur. Phys. J. C 80 (2020), no. 2 83, [arXiv:1807.01955].
- [23] J. R. Forshaw, J. Holguin, and S. Plätzer, Parton branching at amplitude level, JHEP 08 (2019) 145, [arXiv:1905.08686].
- [24] G. Corcella, I. G. Knowles, G. Marchesini, S. Moretti, K. Odagiri, P. Richardson, M. H. Seymour, and B. R. Webber, HERWIG 6: An Event generator for hadron emission reactions with interfering gluons (including supersymmetric processes), JHEP 01 (2001) 010, [hep-ph/0011363].
- [25] A. Karlberg, G. P. Salam, L. Scyboz, and R. Verheyen, Spin correlations in final-state parton showers and jet observables, Eur. Phys. J. C 81 (2021), no. 8 681, [arXiv:2103.16526].
- [26] K. Hamilton, A. Karlberg, G. P. Salam, L. Scyboz, and R. Verheyen, *Soft spin correlations in final-state parton showers*, *JHEP* **03** (2022) 193, [arXiv:2111.01161].
- [27] G. Bewick et al., Herwig 7.3 release note, Eur. Phys. J. C 84 (2024), no. 10 1053, [arXiv:2312.05175].
- [28] S. Höche, M. Hoppe, and D. Reichelt, A simple algorithm for polarized parton evolution, arXiv: 2508.19018.
- [29] A. Majumder and M. Van Leeuwen, The Theory and Phenomenology of Perturbative QCD Based Jet Quenching, Prog. Part. Nucl. Phys. 66 (2011) 41–92, [arXiv:1002.2206].
- [30] Y. Mehtar-Tani, J. G. Milhano, and K. Tywoniuk, Jet physics in heavy-ion collisions, Int. J. Mod. Phys. A 28 (2013) 1340013, [arXiv:1302.2579].

- [31] J.-P. Blaizot and Y. Mehtar-Tani, Jet Structure in Heavy Ion Collisions, Int. J. Mod. Phys. E 24 (2015), no. 11 1530012, [arXiv:1503.05958].
- [32] M. Connors, C. Nattrass, R. Reed, and S. Salur, Jet measurements in heavy ion physics, Rev. Mod. Phys. 90 (2018) 025005, [arXiv:1705.01974].
- [33] L. Cunqueiro and A. M. Sickles, Studying the QGP with Jets at the LHC and RHIC, Prog. Part. Nucl. Phys. 124 (2022) 103940, [arXiv:2110.14490].
- [34] L. Apolinário, Y.-J. Lee, and M. Winn, Heavy quarks and jets as probes of the QGP, Prog. Part. Nucl. Phys. 127 (2022) 103990, [arXiv:2203.16352].
- [35] L. Apolinário, Y.-T. Chien, and L. Cunqueiro Mendez, Jet substructure, Int. J. Mod. Phys. E 33 (2024), no. 07 2430003.
- [36] X.-N. Wang and U. A. Wiedemann, QGP@50: More than Four Decades of Jet Quenching, 8, 2025. arXiv:2508.18794.
- [37] R. Baier, Y. L. Dokshitzer, A. H. Mueller, S. Peigne, and D. Schiff, Radiative energy loss of high-energy quarks and gluons in a finite volume quark - gluon plasma, Nucl. Phys. B 483 (1997) 291–320, [hep-ph/9607355].
- [38] B. G. Zakharov, Fully quantum treatment of the Landau-Pomeranchuk-Migdal effect in QED and QCD, JETP Lett. 63 (1996) 952–957, [hep-ph/9607440].
- [39] U. A. Wiedemann, Gluon radiation off hard quarks in a nuclear environment: Opacity expansion, Nucl. Phys. B 588 (2000) 303-344, [hep-ph/0005129].
- [40] A. Ipp, D. I. Müller, and D. Schuh, Anisotropic momentum broadening in the 2+1D Glasma: analytic weak field approximation and lattice simulations, Phys. Rev. D 102 (2020), no. 7 074001, [arXiv:2001.10001].
- [41] M. E. Carrington, A. Czajka, and S. Mrowczynski, Jet quenching in glasma, Phys. Lett. B 834 (2022) 137464, [arXiv:2112.06812].
- [42] J. Barata, S. Hauksson, X. Mayo López, and A. V. Sadofyev, Jet quenching in the glasma phase: medium-induced radiation, arXiv:2406.07615.
- [43] D. Avramescu, V. Greco, T. Lappi, H. Mäntysaari, and D. Müller, Impact of glasma on heavy flavor azimuthal correlations and spectra, Phys. Rev. D 111 (2025), no. 7 074036, [arXiv:2409.10564].
- [44] D. Avramescu, V. Greco, T. Lappi, H. Mäntysaari, and D. Müller, Heavy-Flavor Angular Correlations as a Direct Probe of the Glasma, Phys. Rev. Lett. 134 (2025), no. 17 172301, [arXiv:2409.10565].
- [45] K. Boguslavski, A. Kurkela, T. Lappi, F. Lindenbauer, and J. Peuron, Jet momentum broadening during initial stages in heavy-ion collisions, Phys. Lett. B 850 (2024) 138525, [arXiv:2303.12595].
- [46] K. Boguslavski, A. Kurkela, T. Lappi, F. Lindenbauer, and J. Peuron, Jet quenching parameter in QCD kinetic theory, Phys. Rev. D 110 (2024), no. 3 034019, [arXiv:2312.00447].
- [47] A. Altenburger, K. Boguslavski, and F. Lindenbauer, Jet broadening and radiation in the early anisotropic plasma in heavy-ion collisions, arXiv:2509.03868.
- [48] J. Barata, K. Boguslavski, F. Lindenbauer, and A. V. Sadofyev, *Jet quenching in out-of-equilibrium QCD matter*, arXiv:2511.07519.

- [49] A. V. Sadofyev, M. D. Sievert, and I. Vitev, Ab initio coupling of jets to collective flow in the opacity expansion approach, Phys. Rev. D 104 (2021), no. 9 094044, [arXiv:2104.09513].
- [50] L. Antiporda, J. Bahder, H. Rahman, and M. D. Sievert, Jet drift and collective flow in heavy-ion collisions, Phys. Rev. D 105 (2022), no. 5 054025, [arXiv:2110.03590].
- [51] J. Barata, A. V. Sadofyev, and C. A. Salgado, Jet broadening in dense inhomogeneous matter, Phys. Rev. D 105 (2022), no. 11 114010, [arXiv:2202.08847].
- [52] C. Andres, F. Dominguez, A. V. Sadofyev, and C. A. Salgado, Jet broadening in flowing matter: Resummation, Phys. Rev. D 106 (2022), no. 7 074023, [arXiv:2207.07141].
- [53] Y. Fu, J. Casalderrey-Solana, and X.-N. Wang, Asymmetric transverse momentum broadening in an inhomogeneous medium, Phys. Rev. D 107 (2023), no. 5 054038, [arXiv:2204.05323].
- [54] J. Barata, X. Mayo López, A. V. Sadofyev, and C. A. Salgado, Medium induced gluon spectrum in dense inhomogeneous matter, Phys. Rev. D 108 (2023), no. 3 034018, [arXiv:2304.03712].
- [55] J. Barata, J. G. Milhano, and A. V. Sadofyev, Picturing QCD jets in anisotropic matter: from jet shapes to energy energy correlators, Eur. Phys. J. C 84 (2024), no. 2 174, [arXiv:2308.01294].
- [56] M. V. Kuzmin, X. Mayo López, J. Reiten, and A. V. Sadofyev, Jet quenching in anisotropic flowing matter, Phys. Rev. D 109 (2024), no. 1 014036, [arXiv:2309.00683].
- [57] M. V. Kuzmin and X. Mayo López, Gluon radiation inside a flowing medium, arXiv:2406.14628.
- [58] W. Ke, J. Terry, and I. Vitev, Anisotropic jet broadening and jet shape, JHEP 07 (2025) 097, [arXiv:2412.12250].
- [59] S. Hauksson, S. Jeon, and C. Gale, Momentum broadening of energetic partons in an anisotropic plasma, Phys. Rev. C 105 (2022), no. 1 014914, [arXiv:2109.04575].
- [60] S. Hauksson and E. Iancu, Jet polarisation in an anisotropic medium, JHEP 08 (2023) 027, [arXiv:2303.03914].
- [61] J. Barata, C. A. Salgado, and J. M. Silva, Gluon to $q\overline{q}$ antenna in anisotropic QCD matter: spin-polarized and azimuthal jet observables, JHEP 12 (2024) 023, [arXiv:2407.04774].
- [62] J. Barata, J. Brewer, K. Lee, and J. M. Silva, Heavy Quark Pair Energy Correlators: From Profiling Partonic Splittings to Probing Heavy-Flavor Fragmentation, arXiv:2508.19404.
- [63] Y. Mehtar-Tani, C. A. Salgado, and K. Tywoniuk, Anti-angular ordering of gluon radiation in QCD media, Phys. Rev. Lett. 106 (2011) 122002, [arXiv:1009.2965].
- [64] Y. Mehtar-Tani, C. A. Salgado, and K. Tywoniuk, Jets in QCD Media: From Color Coherence to Decoherence, Phys. Lett. B 707 (2012) 156–159, [arXiv:1102.4317].
- [65] J. Casalderrey-Solana and E. Iancu, Interference effects in medium-induced gluon radiation, JHEP 08 (2011) 015, [arXiv:1105.1760].
- [66] Y. Mehtar-Tani and K. Tywoniuk, Jet coherence in QCD media: the antenna radiation spectrum, JHEP 01 (2013) 031, [arXiv:1105.1346].
- [67] Y. Mehtar-Tani, C. A. Salgado, and K. Tywoniuk, The radiation pattern of a QCD antenna in a dilute medium, JHEP 04 (2012) 064, [arXiv:1112.5031].

- [68] N. Armesto, H. Ma, Y. Mehtar-Tani, C. A. Salgado, and K. Tywoniuk, Coherence effects and broadening in medium-induced QCD radiation off a massive qq antenna, JHEP 01 (2012) 109, [arXiv:1110.4343].
- [69] Y. Mehtar-Tani, C. A. Salgado, and K. Tywoniuk, The Radiation pattern of a QCD antenna in a dense medium, JHEP 10 (2012) 197, [arXiv:1205.5739].
- [70] J. Casalderrey-Solana, Y. Mehtar-Tani, C. A. Salgado, and K. Tywoniuk, New picture of jet quenching dictated by color coherence, Phys. Lett. B 725 (2013) 357–360, [arXiv:1210.7765].
- [71] M. R. Calvo, M. R. Moldes, and C. A. Salgado, Color coherence in a heavy quark antenna radiating gluons inside a QCD medium, Phys. Lett. B 738 (2014) 448–452, [arXiv:1403.4892].
- [72] J. Barata, F. Domínguez, C. A. Salgado, and V. Vila, A modified in-medium evolution equation with color coherence, JHEP 05 (2021) 148, [arXiv:2101.12135].
- [73] S. Abreu, X. Mayo López, G. Milhano, and A. Soto-Ontoso, A generalized picture of colour decoherence in dense QCD media, JHEP 03 (2025) 216, [arXiv:2410.24135].
- [74] C. Andres, L. Apolinário, N. Armesto, A. Cordeiro, F. Dominguez, P. Guerrero-Rodríguez, and J. G. Milhano, Gluon emission by a qq̄ antenna with realistic parton-medium interactions, in 31st International Conference on Ultra-relativistic Nucleus-Nucleus Collisions, 8, 2025. arXiv:2508.21719.
- [75] M. V. Kuzmin and J. M. Silva, QCD antenna radiative spectrum in dense media: accounting for full jet-medium interactions, arXiv:2507.00143.
- [76] M. Fickinger, G. Ovanesyan, and I. Vitev, Angular distributions of higher order splitting functions in the vacuum and in dense QCD matter, JHEP 07 (2013) 059, [arXiv:1304.3497].
- [77] J. Casalderrey-Solana, D. Pablos, and K. Tywoniuk, Two-gluon emission and interference in a thin QCD medium: insights into jet formation, JHEP 11 (2016) 174, [arXiv:1512.07561].
- [78] P. Arnold and S. Iqbal, The LPM effect in sequential bremsstrahlung, JHEP 04 (2015) 070, [arXiv:1501.04964]. [Erratum: JHEP 09, 072 (2016)].
- [79] P. Arnold, O. Elgedawy, and S. Iqbal, Are Gluon Showers inside a Quark-Gluon Plasma Strongly Coupled? A Theorist's Test, Phys. Rev. Lett. 131 (2023), no. 16 162302, [arXiv:2212.08086].
- [80] P. Arnold, O. Elgedawy, and S. Iqbal, Landau-Pomeranchuk-Migdal effect in sequential bremsstrahlung: Gluon shower development, Phys. Rev. D 108 (2023), no. 7 074015, [arXiv:2302.10215].
- [81] P. Arnold, O. Elgedawy, and S. Iqbal, Are in-medium quark-gluon showers strongly coupled? results in the large-N_f limit, JHEP **01** (2025) 193, [arXiv:2408.07129].
- [82] H. Chen, I. Moult, and H. X. Zhu, Quantum Interference in Jet Substructure from Spinning Gluons, Phys. Rev. Lett. 126 (2021), no. 11 112003, [arXiv:2011.02492].
- [83] Y.-K. Song, S.-Y. Wei, L. Yang, and J. Zhou, Gluon Polarimetry with Energy-Energy Correlators, arXiv:2509.14960.

- [84] F. Domínguez, J. G. Milhano, C. A. Salgado, K. Tywoniuk, and V. Vila, Mapping collinear in-medium parton splittings, Eur. Phys. J. C 80 (2020), no. 1 11, [arXiv:1907.03653].
- [85] J. H. Isaksen and K. Tywoniuk, Wilson line correlators beyond the large-N_c, JHEP 21 (2020) 125, [arXiv:2107.02542].
- [86] S. Keller and E. Laenen, Next-to-leading order cross-sections for tagged reactions, Phys. Rev. D 59 (1999) 114004, [hep-ph/9812415].
- [87] S. Catani, S. Dittmaier, and Z. Trocsanyi, One loop singular behavior of QCD and SUSY QCD amplitudes with massive partons, Phys. Lett. B 500 (2001) 149–160, [hep-ph/0011222].
- [88] P. K. Dhani, G. Rodrigo, and G. F. R. Sborlini, *Triple-collinear splittings with massive particles*, *JHEP* 12 (2023) 188, [arXiv:2310.05803].
- [89] E. Craft, M. Gonzalez, K. Lee, B. Mecaj, and I. Moult, The 1 → 3 massive splitting functions from QCD factorization and SCET, JHEP 07 (2024) 080, [arXiv:2310.06736].
- [90] G. Somogyi, Z. Trocsanyi, and V. Del Duca, Matching of singly- and doubly-unresolved limits of tree-level QCD squared matrix elements, JHEP 06 (2005) 024, [hep-ph/0502226].
- [91] O. Braun-White and N. Glover, Decomposition of triple collinear splitting functions, JHEP 09 (2022) 059, [arXiv:2204.10755].
- [92] J. H. Isaksen and K. Tywoniuk, *Precise description of medium-induced emissions*, *JHEP* **09** (2023) 049, [arXiv:2303.12119].
- [93] Y. Mehtar-Tani, The Physics of Jet Quenching in Perturbative QCD, arXiv:2509.26394.
- [94] X.-N. Wang, M. Gyulassy, and M. Plumer, The LPM effect in QCD and radiative energy loss in a quark gluon plasma, Phys. Rev. D 51 (1995) 3436–3446, [hep-ph/9408344].
- [95] J.-P. Blaizot, F. Dominguez, E. Iancu, and Y. Mehtar-Tani, Medium-induced gluon branching, JHEP 01 (2013) 143, [arXiv:1209.4585].
- [96] L. D. McLerran and R. Venugopalan, Computing quark and gluon distribution functions for very large nuclei, Phys. Rev. D 49 (1994) 2233–2241, [hep-ph/9309289].
- [97] M. Gyulassy and X.-n. Wang, Multiple collisions and induced gluon Bremsstrahlung in QCD, Nucl. Phys. B 420 (1994) 583-614, [nucl-th/9306003].
- [98] F. Dominguez, C. Marquet, B.-W. Xiao, and F. Yuan, *Universality of Unintegrated Gluon Distributions at small x, Phys. Rev. D* 83 (2011) 105005, [arXiv:1101.0715].
- [99] F. Dominguez, C. Marquet, A. M. Stasto, and B.-W. Xiao, Universality of multiparticle production in QCD at high energies, Phys. Rev. D 87 (2013) 034007, [arXiv:1210.1141].
- [100] L. Apolinário, N. Armesto, J. G. Milhano, and C. A. Salgado, Medium-induced gluon radiation and colour decoherence beyond the soft approximation, JHEP 02 (2015) 119, [arXiv:1407.0599].
- [101] H. Kleinert, Path Integrals in Quantum Mechanics, Statistics, Polymer Physics, and Financial Markets, .
- [102] CMS Collaboration, Measurement of gluon spin effect in parton splittings, .
- [103] Z. Citron et al., Report from Working Group 5: Future physics opportunities for high-density QCD at the LHC with heavy-ion and proton beams, CERN Yellow Rep. Monogr. 7 (2019) 1159-1410, [arXiv:1812.06772].

- [104] W.-H. Yao, X. Li, H. Dong, and S.-Y. Wei, Quenching of polarized jets, arXiv:2511.06705.
- [105] J. Barata, I. Moult, A. V. Sadofyev, and J. M. Silva, Dissecting Jet Modification in the QGP with Multi-Point Energy Correlators, arXiv:2503.13603.
- [106] F. Cougoulic and Y. V. Kovchegov, Helicity-dependent extension of the McLerran-Venugopalan model, Nucl. Phys. A 1004 (2020) 122051, [arXiv:2005.14688].
- [107] H. C. Pauli, A compendium of light cone quantization, Nucl. Phys. B Proc. Suppl. 90 (2000) 259–272, [hep-ph/0103106].
- [108] Y. V. Kovchegov and E. Levin, *Quantum Chromodynamics at High Energy*, vol. 33. Oxford University Press, 2013.
- [109] T. Lappi and R. Paatelainen, The one loop gluon emission light cone wave function, Annals Phys. 379 (2017) 34–66, [arXiv:1611.00497].